MULTIUSER RECEIVERS FOR CDMA DOWNLINK

A THESIS SUBMITTED TO
THE GRADUATE SCHOOL OF NATURAL AND APPLIED SCIENCES
OF
MIDDLE EAST TECHNICAL UNIVERSITY

BY

ÖMER AGAH DURAN

IN PARTIAL FULFILLMENT OF THE REQUIREMENTS
FOR
THE DEGREE OF MASTER OF SCIENCE
IN
ELECTRICAL AND ELECTRONICS ENGINEERING

AUGUST 2008

Approval of the thesis:

MULTIUSER RECEIVERS FOR CDMA DOWNLINK

submitted by **ÖMER AGAH DURAN** in partial fulfillment of the requirements for the degree of **Master of Science in Electrical and Electronics Engineering Department, Middle East Technical University** by,

Prof. Dr. Canan Özgen
Dean, Graduate School of **Natural and Applied Sciences** _____

Prof. Dr. İsmet Erkmen
Head of Department, **Electrical and Electronics Engineering** _____

Assist. Prof. Dr. Çağatay Candan
Supervisor, **Electrical and Electronics Eng. Dept., METU** _____

Examining Committee Members:

Prof. Dr. Yalçın Tanık
Electrical and Electronics Engineering Dept., METU _____

Assist. Prof. Dr. Çağatay Candan
Electrical and Electronics Engineering Dept., METU _____

Prof. Dr. Gözde Bozdağı Akar
Electrical and Electronics Engineering Dept., METU _____

Assist. Prof. Dr. A. Özgür Yılmaz
Electrical and Electronics Engineering Dept., METU _____

Ercan Şut, M.Sc.
ASELSAN Inc. _____

Date: 27.08.2008

I hereby declare that all information in this document has been obtained and presented in accordance with academic rules and ethical conduct. I also declare that, as required by these rules and conduct, I have fully cited and referenced all material and results that are not original to this work.

Name, Last Name: Ömer Agah Duran

Signature:

ABSTRACT

MULTIUSER RECEIVERS FOR CDMA DOWNLINK

Duran, Ömer Agah
M. Sc., Department of Electrical and Electronics Engineering
Supervisor: Assist. Prof. Dr. Çağatay Candan

August 2008, 78 pages

In this thesis, multiuser receivers for code division multiple-access (CDMA) downlink are studied under frequency selective fading channel conditions. The receivers investigated in this thesis attempt to estimate desired symbol as a linear combination of chip-rate sampled received signal sequence. A common matrix-vector representation of signals, which is similar to the model given by Paulraj *et. al.* is constructed in order to analyze the receivers studied in this thesis.

Two receivers already well known in the literature are introduced and derived by using the common signal model. One of the receivers uses traditional matched filter and the other uses symbol-level linear minimum mean square error (MMSE) estimation. The receiver that uses traditional matched filter, also known as the conventional RAKE receiver, benefits from time diversity by combining the signal energy from multiple paths. The conventional RAKE receiver is optimal when multiple-access interference (MAI) is absent. Linear MMSE based receivers are known to suppress MAI and to be more robust to noise enhancement. The optimal

symbol-level linear MMSE based receiver requires inversion of large matrices whose size is determined by either number of active users or spreading factor. These two parameters can be quite large in many practical systems and hence the computational load of this receiver can be a problem.

In this thesis, two alternative low-complexity receivers, which are chip-level linear MMSE equalizer proposed by Krauss *et. al.* and interference-suppressing RAKE receiver proposed by Paulraj *et. al.*, are compared with the linear full-rank MMSE based receiver and with the conventional RAKE receiver in terms of bit-error-rate performance. Various simulations are performed to evaluate the performance of the receivers and the parameters affecting the receiver performance are investigated.

Keywords: CDMA downlink, multiuser receiver, interference-suppressing RAKE, symbol-level linear MMSE estimation, chip-level linear MMSE equalizer.

ÖZ

CDMA UYDU-YER BAĞI İÇİN ÇOK KULLANICILI ALMAÇLAR

Duran, Ömer Agah

Yüksek Lisans, Elektrik ve Elektronik Mühendisliği Bölümü

Tez Yöneticisi: Yard. Doç. Dr. Çağatay Candan

Ağustos 2008, 78 sayfa

Bu tez çalışmasında, kod bölmeli çoklu erişim (CDMA) uydu-yer bağı yönünde çok kullanıcılı almaçlar frekansa bağımlı sönümlemeli kanal durumları altında incelenmiştir. Bu tezde incelenen almaçlar istenen sembolü chip-düzeyi örneklenmiş alınan sinyal dizisinin doğrusal bir birleşimi olarak kestirmeye çalışmaktadır. Bu tezde incelenen almaçların çözümlemesinin yapılması için Paulraj tarafından verilen modele benzer ortak bir matris-vektör gösterimi oluşturulmuştur.

Literatürde iyi bilinen iki almaç tanıtılmış ve ortak sinyal modeli kullanılarak elde edilmiştir. Almaçlardan biri alışılagelmiş uyumlu süzgeç diğeri ise sembol-düzeyi doğrusal en küçük karesel ortalama hata (MMSE) kestirimi kullanmaktadır. Alışılagelmiş uyumlu süzgeç kullanan almaç, başka bir deyişle geleneksel RAKE almaç, çok yollu gelen işaretlerin enerjilerini birleştirerek zaman çeşitlemesinden yararlanmaktadır. Çoklu erişim girişimi (MAI) olmadığı durumda, RAKE almaç en iyidir. Doğrusal MMSE kullanan almaçların MAI'yı bastırabildiği ve gürültü değerinin yükseltilmesine karşı daha dayanıklı olduğu bilinmektedir. En iyi sembol-

düzeyi doğrusal MMSE kullanan almaçta, boyutu etkin kullanıcı sayısı veya yayılım etkeni ile belirlenen daha büyük matrislerin tersinin alınması gerekmektedir. Bu iki parametre, birçok uygulanabilir sistemde oldukça büyük değerlere sahip olabilir ve bu durum daha fazla işlem karmaşıklığı gerektirmektedir.

Bu tez çalışmasında; Krauss tarafından önerilen chip-düzeyi doğrusal MMSE denkleştirici ve Paulraj tarafından önerilen girişim-bastırıcı RAKE almaç gibi iki alternatif az karmaşık almaç, tam-kerteli MMSE kullanan almaç ve geleneksel RAKE almaç ile bit hata oranı başarımı açısından karşılaştırılmıştır. Almaçların başarımını değerlendirmek için çeşitli simülasyonlar yapılmış ve almaç başarımı üzerinde etkisi olan parametreler incelenmiştir.

Anahtar sözcükler: CDMA uydu-yer bağı, çok kullanıcılı almaç, girişim-bastırıcı RAKE, sembol-düzeyi doğrusal MMSE kestirimi, chip-düzeyi doğrusal MMSE denkleştirici.

To My Family

ACKNOWLEDGMENTS

First, I wish to express my deepest gratitude to my supervisor Assist. Prof. Dr. Çağatay Candan for his guidance, advice, criticism, encouragements and insight throughout the research.

I would also like to thank to all my friends and colleagues who contributed to the completion of this thesis with their suggestions, comments and encouragements.

I would especially like to express my deepest appreciation to my family for their continuous support throughout this thesis study.

TABLE OF CONTENTS

LIST OF TABLES

TABLES

LIST OF FIGURES

FIGURES

LIST OF ABBREVIATIONS

AWGN	:	Additive White Gaussian Noise
BEP	:	Bit Error Probability
BER	:	Bit Error Rate
BLS	:	Bayes' Least-Squares
CDMA	:	Code Division Multiple-Access
DFE	:	Decision-Feedback Equalizer
DS/CDMA	:	Direct-Sequence CDMA
EGC	:	Equal-Gain Combining
FH/CDMA	:	Frequency-Hopping CDMA
ICI	:	Interchip Interference
ISI	:	Intersymbol Interference
IS-RAKE	:	Interference-Suppressing RAKE
LMMSE	:	Linear Minimum Mean Square Error
MAI	:	Multiple-Access Interference
MLSD	:	Maximum Likelihood Sequence Detector
MMSE	:	Minimum Mean Square Error
MRC	:	Maximal Ratio Combining
MSE	:	Mean Square Error
SC	:	Selection Combining
SINR	:	Signal-to-Interference-plus-Noise Ratio
SNR	:	Signal-to-Noise Ratio
UWB	:	Ultra Wide Band
ZF	:	Zero-Forcing

CHAPTER 1

INTRODUCTION

Although it has received more attention in the last decades, spread-spectrum systems have a long history in wireless communication. Spread-spectrum systems are used in a wide application area because of its desirable properties such as robustness to jamming and interference, resistance to interception by unintended receiver, frequency reuse and suitability for multiple-access communication [1], [2]. A spread-spectrum signal employs a transmission bandwidth much larger than the transferred data rate. Each sample period in spreading sequence is called a chip and the ratio of symbol period to chip period is called spreading factor. Spreading of the transmitted signal in the spectrum appears to be unfavorable for spectral efficiency, however among wireless communication systems using different multiple-access techniques, spread-spectrum systems have a number of advantages in today's wireless communication applications. Spreading factor is also called processing gain since the maximum number of allocated users in a common spectrum, the amount of tolerable interference, etc. are proportional to spreading factor.

1.1. CDMA Systems

Code division multiple-access (CDMA) is the technique that uses spread spectrum modulation by assigning different spreading sequences in direct-sequence CDMA (DS/CDMA) or different frequency hopping patterns in frequency-hopping CDMA (FH/CDMA) to each user. Direct-sequence denotes that the spread-spectrum signal is

transmitted as a product of user data and the spreading sequence [2]. Spreading waveform of single user can be represented as

$$c(t) = \sum_{n=-\infty}^{\infty} c[n]\, p(t - nT_c) \tag{1-1}$$

where $c[n]$ represents a chip which is assumed to be either +1 or -1 in this thesis. In this thesis, we use bi-phase codes such as Walsh-Hadamard codes. Any other polyphase codes can also be used. The function p(t) is the pulse shape used in the transmission with chip period T_c. The baseband equivalent transmitted signal $x(t)$ can be expressed as

$$x(t) = c(t)\, s(t) \tag{1-2}$$

where $s(t)$ denotes the user data.

DS/CDMA systems can use orthogonal spreading sequences to accommodate many users in a common spectrum. However, in a multipath (or frequency-selective) propagation channel, the delayed copies of transmitted multiuser signal destroy the orthogonality of spreading sequences. In addition, fading of the channel results in poor signals to be captured at the receiver. These two problems can be handled by applying several modulation and demodulation methods along with additional digital signal processing. In this thesis, the receiver side of multiuser CDMA communication under multipath propagation channels is of interest. In particular, downlink or forward link communication, i.e. from base station to mobile, has some useful properties that may increase the chance of truthful extraction of the desired signal from multiuser signal. This thesis work, hence, focuses on CDMA downlink receivers.

1.2. CDMA Downlink Receivers

CDMA downlink receivers are designed to combat both the signal distortion due to multipath (also known as the signal dispersion) and the reduction of instantaneous signal power due to the random nature of the channel.

A CDMA downlink method is based on utilizing time diversity to collect energy from several paths. The conventional receiver, which is called RAKE receiver, weights the signals from different paths with some coefficients and combines them to produce a decision variable. The inverse operation of the spreading, which is called despreading, can be performed either prior to or after weighting the signal strength of the branches. In this thesis, we examine the postdetection maximal ratio combining (MRC) method, a particular solution of RAKE, that first despreading and then MRC is performed. MRC is applied selecting the receiver coefficients by matching the channel coefficients.

A second approach is based on eliminating the interference caused by multipath signals by applying the linear estimation theory for channel equalization. The optimal weight vector of receiver performing linear operations on received sampled data for a given observation window can be derived considering mean square error (MSE) estimation. The optimal linear estimator uses a filter whose size is equal to or larger than the observation window, which is typically a single symbol period. Minimizing the MSE over sufficiently large observation window, it is called full-rank linear minimum mean square error (LMMSE) receiver.

In addition to two mentioned methods, two other receivers based on MMSE method are investigated as an essential part of this thesis work. These two newer methods also benefit from the good properties of CDMA downlink communication and both are considered as low-complexity receivers, which are alternative to full-rank LMMSE receiver. One is based on chip-level equalization [13]. This receiver first

performs chip-level equalization of the channel to reduce the interference caused by multipath considering MSE criterion, and then applies despreading to obtain symbol estimation. The second receiver has a RAKE structure but differs from conventional method in selection of tap weights and the number of taps for interference suppression [14]. This new interference-suppressing RAKE first applies despreading for several delayed copies of the received signal and then combines the output of the despreading with the weights calculated based on MSE criterion at symbol-level.

The operation order where despreading takes place in the estimation of the symbol, yields different receiver structure with different combining weights. In particular, the full-rank LMMSE performs a more general combining method with large number of taps covering a wide observation window instead of directly despreading the received signal by desired user's spreading sequence. Hence, the level of the interference suppression and the receiver performance, which depends on received signal parameters and the order of operations, are examined in the scope of this thesis.

One of the objectives of this thesis work is to evaluate the performance of the receivers, which are examined in the scope of this study, with the aid of the simulations and to compare the receivers exploiting the different aspects of the simulation results.

In this thesis, all three MMSE based receivers are derived by using a similar signal model given in [14] to construct a base for more accurate comparison and analysis of the receivers. In the analysis of concerned receivers, the parameters that characterize the transmitted multiuser signal are assumed to be known to give a more detailed comparison while the implementation can be realized using training symbols.

The studies on CDMA receivers involve different system designs and environments. In contrast to downlink, the uplink (reverse link) channel has some difficulties such

as asynchronous transmission, separate channels of each user with different characterization. The receivers that concentrate on uplink communication are still an interesting research area [21]. If the system parameters and user parameters are unknown, some blind methods are proposed [22]. Similar studies also performed in Ultra wide band (UWB) systems [23] .

1.3. Organization of Thesis

This thesis work is organized as follows:

Chapter 2 follows the introduction chapter and a general mathematical modeling of CDMA downlink is constructed. Construction method is explained considering discrete-time model. Some design parameters are also given.

In Chapter 3, a detailed analysis of the mentioned CDMA downlink receivers, which use linear operations for estimation of desired symbol, is performed. Structures of the analyzed receivers and effects of the design parameters are discussed.

Chapter 4 presents the simulation results of four different CDMA downlink receivers examined in Chapter 3. The performance evaluation of the receivers are performed considering different system and receiver parameters.

Finally, in Chapter 5, the thesis work is summarized with the explanations of the results obtained from the study on multiuser receivers for the CDMA downlink.

CHAPTER 2

MATHEMATICAL MODELING OF MULTIUSER COMMUNICATION IN DS-CDMA SYSTEMS

In this chapter, a general system model is constructed which is used in the modeling of the receivers that will be derived in next chapter. This system model will provide more accurate analysis and comparison of performances of the different receivers. Time domain representations of signals will be more suitable for the calculations and derivations of the general system model.

A basic functional discrete-time model of DS-CDMA downlink with BPSK is depicted in Figure 2-1. Both sides of this model, transmitter and receiver, may be suitable to perform additional signal processing in order to improve the ability of making correct decision. Throughout this work, unless otherwise stated it has been considered that transmitter side performs basics of data transmission without any further pre-processing or post-processing. Data symbols in transmitter side are binary data or bits transferred from previous stages of device after required processing.

This chapter focuses on the general structure of transmission and reception of the user data. Section 2.1 explains the basic model of the transmitted signal. Section 2.2 represents the received signal in a suitable form for detection. Finally, Section 2.3 presents the discrete-time modeling of the received signal. Furthermore, this section constructs the matrix and vector form of the received signal.

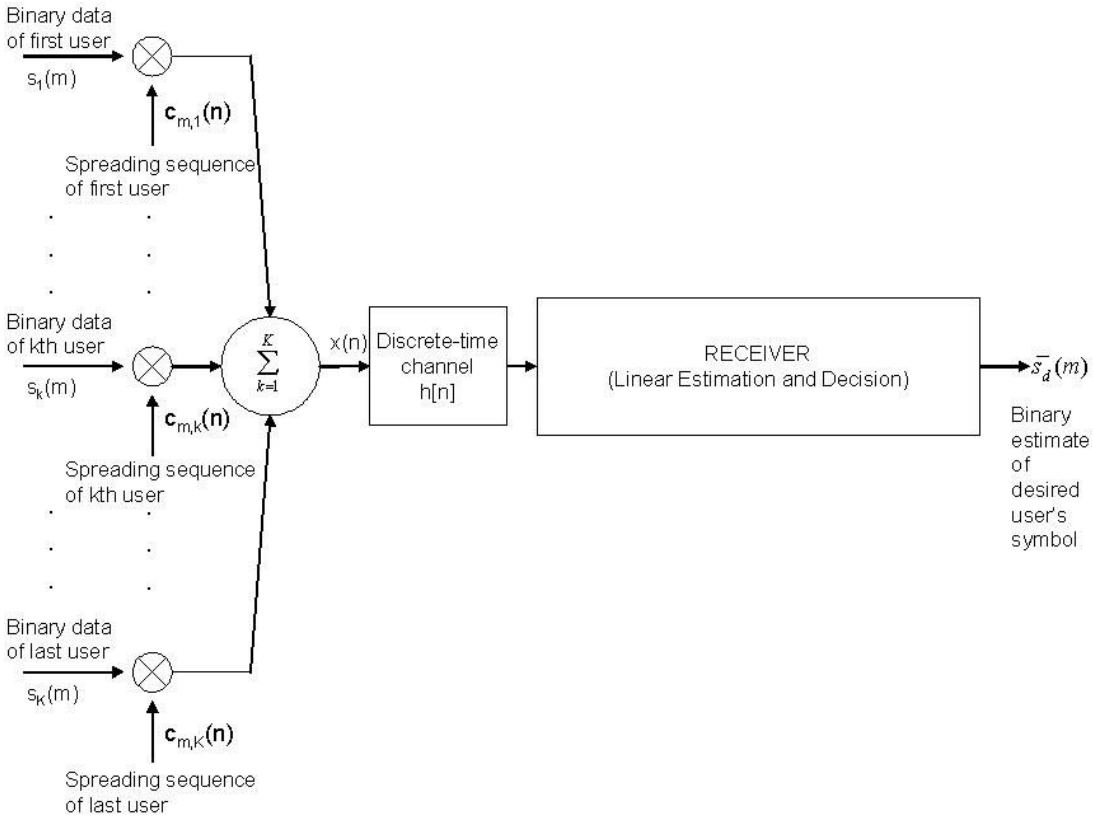

Figure 2-1: A basic discrete-time model of DS-CDMA downlink with BPSK

2.1. Transmitted Signal Model

In this section, a real-valued baseband equivalent model of transmitter is used assuming that base station has symbol synchronization for different users and uses BPSK modulation. K is the number of active users in the cell. The m th binary data symbol for user k is denoted as $s_k[m]$ and it is spread using the symbol-period-dependent chip sequence of k th user $\{ c_{m,k}[n] \}_{n=0}^{N-1}$ which is assumed that it can take value from $\{\pm 1\}$ in this study. Chip index is denoted as n and N is spreading factor

or processing gain. The term "symbol-period-dependent" means that the spreading sequence of a user is product of a periodic orthogonal code (such as Walsh-Hadamard code) and an aperiodic pseudo-random scrambling code (such as base station dependent short pseudo-random code used in IS-95 system). The transmitted sum signal of all the users from a known base station, so called "multiuser chip symbol", $x[n]$ can be expressed as

$$x[n] = \sum_{k=1}^{K} A_k \, s_k[m] c_{m,k}[n \ Mod \ N] \tag{2-1}$$

$$= \sum_{k=1}^{K} A_k \, s_k[\lfloor n/N \rfloor] c_{\lfloor n/N \rfloor,k}[n \ Mod \ N] \tag{2-2}$$

where A_k is k th user amplitude. The operation $\lfloor a \rfloor$ rounds a to the nearest integer less than or equal to a.

The baseband discrete-time signal $x[n]$ is modulated by a pulse satisfying Nyquist criterion. After waveshaping or chip pulse shaping filter, it is obtained:

$$x(t) = \sum_{n=-\infty}^{\infty} x[n] p(t - nT_c) \quad -\infty < t < \infty \tag{2-3}$$

where $p(t)$ is the chip waveform and $1/T_c$ is chip rate or T_c is chip duration. In general, the chip waveform $p(t)$ is not limited to time interval $[0, T_c]$. The energy per chip E_c can be calculated as in (2-4).

$$\int_{-\infty}^{\infty} \left| p(t)^2 \right| dt = E_c \tag{2-4}$$

2.2. Received Signal Model

The baseband equivalent transmitted signal given in Equation (2-3) is assumed to pass through a dispersive multipath propagation channel. The multipath propagation channel can be expressed as

$$h(t) = \sum_{l=0}^{L-1} h_l \, \delta(t - \tau_l) \tag{2-5}$$

where l denotes channel path index. τ_l and h_l are the delay for the l th path and the complex-valued channel coefficient, respectively. L is the number of resolvable paths. In this case, since wideband channel is used for transmission, we can say two multipath signals are resolvable [4] if the time difference between two delays is larger than chip period T_c :

$$\left|\tau_i - \tau_j\right| > T_c \quad 0 \le i.j \le L-1, i \ne j \tag{2-6}$$

The baseband equivalent received signal can be expressed as convolution of transmitted signal and channel impulse response under additive noise:

$$r(t) = \sum_{l=0}^{L-1} h_l \, x(t - \tau_l) + \eta(t) \tag{2-7}$$

where $\eta(t)$ denotes total zero-mean noise with autocorrelation $R_{nn}(\tau) = \int_{-\infty}^{\infty} \eta(t)\eta^*(t-\tau)dt$.

After the matched pulse shaping filter, output of the filter can be expressed as:

$$y(t) = \int_{-\infty}^{\infty} r(\tau) p^*(t-\tau) d\tau \tag{2-8}$$

2.3. Discrete-Time Model of Received Signal

Detection of transmitted user information or bits requires discrete-time signal processing of received signal. In order to form a set of useful discrete data for estimation of multiuser chip symbol, output of the pulse shaping matched filter is sampled at chip rate $1/T_c$ as in Figure 2-1. The discrete time model of input signal may be written as

$$y[n] = \sum_{l=0}^{L-1} h_l x[n - \tau_l / T_c] + w[n] \tag{2-9}$$

where $w[n]$ is additive zero-mean Gaussian noise with modified power spectral density by the pulse shaping. In (2-9), in order to simplify representation it is assumed that $p(t)$ is unit energy rectangular pulse shape and limited to time interval $[0, T_c]$. Without loss of generality, it can be accepted that τ_l is nonnegative integer multiple of T_c. Since the portion of the interchip interference (ICI) caused by pulse shaping is eliminated with these assumptions, $x[n - \tau_l / T_c]$ represents the exact chip sampled value .

We can express (2-9) in vector form, considering a window of received chip samples whose size is L_w, which is larger than the channel length in general:

$$\mathbf{y} = \mathbf{H} + \mathbf{w} \tag{2-10}$$

where $\mathbf{y}$ is formed stacking L_w received chip samples , $\mathbf{x}$ represents the transmitted $(L_w + L - 1)$ multiuser chips, $\mathbf{w}$ is $L_w \times 1$ noise vector and $\mathbf{H}$ is the $L_w \times (L_w + L - 1)$ channel convolution matrix obtained from $\{h_l\}_{l=0}^{L-1}$ as depicted in (2-11). Continuous stream of chips is transmitted, and hence $\mathbf{H}$ can be constructed regarding contribution of previous chips:

$$\mathbf{H} = \begin{bmatrix} h_{L-1} & h_{L-2} & \cdots & h_0 & 0 & \cdots & 0 & 0 & \cdots & 0 & 0 \\ 0 & h_{L-1} & \cdots & h_1 & h_0 & \cdots & 0 & 0 & \cdots & 0 & 0 \\ \vdots & \vdots & & \vdots & \vdots & & \vdots & \vdots & & \vdots & \vdots \\ \vdots & \vdots & & \vdots & \vdots & & \vdots & \vdots & & \vdots & \vdots \\ 0 & 0 & \cdots & 0 & 0 & \cdots & h_{L-1} & h_{L-2} & \cdots & h_0 & 0 \\ 0 & 0 & \cdots & 0 & 0 & \cdots & 0 & h_{L-1} & \cdots & h_1 & h_0 \end{bmatrix}_{L_w \times (L_w + L - 1)} \tag{2-11}$$

Assuming delay spread of shorter than symbol period T_s , transmitted multiuser chip sequence vector $\mathbf{x}$ can be decomposed as:

$$\mathbf{x} = \mathbf{CAs} \tag{2-12}$$

where

$$\mathbf{C} = [\mathbf{C_1}, \mathbf{C_2}, \ldots, \mathbf{C_K}] \tag{2-13}$$

is $(L_w + L - 1) \times 3K$ three symbol spanning multiuser code matrix, and

$$\mathbf{s} = [\mathbf{s_1}, \mathbf{s_2}, \ldots, \mathbf{s_K}]^{\mathrm{T}} \tag{2-14}$$

is $3K \times 1$ three symbol spanning multiuser symbol vector that single user has $\mathbf{s}_k = [\, s_k[m-1], s_k[m], s_k[m+1] \,]^T$. $\mathbf{A}$ is $3K \times 3K$ diagonal amplitude matrix whose

diagonal entries contain users' signal amplitude. The elements that compose the transmitted multiuser chip sequence have similar structure to those given in [14] except that we use unit amplitude entries by extracting the transmit powers outside the code matrix.

The construction of each $\mathbf{C_k}$ is performed regarding following two statements. Since delay spread is shorter than T_s, observed window spans at most three symbol. Additionally, only periodic orthogonal codes are used in simulations since one base station is assumed. Consequently, $\mathbf{C_k}$ can be formed as:

$$\mathbf{C_k} = \begin{bmatrix} \mathbf{cp}_k & \mathbf{0} & \mathbf{0} \\ \mathbf{0} & \mathbf{c}_k & \mathbf{0} \\ \mathbf{0} & \mathbf{0} & \mathbf{cn}_k \end{bmatrix}_{(L_w+L-1)\times 3} \tag{2-15}$$

where $\mathbf{cp}_k$ represents the interfering chip sequence related to previous symbol and $\mathbf{cn}_k$ represents the interfering chip sequence of next symbol. $\mathbf{cp}_k$ and $\mathbf{cn}_k$ are both obtained from chip sequence of k th user $\mathbf{c}_k$ (symbol index is dropped because of usage of only periodic orthogonal codes) by selecting a truncated sequence from head or end of $\mathbf{c}_k$, respectively. Length of $\mathbf{cp}_k$ and $\mathbf{cn}_k$ are chosen in receiver design so that both lengths are typically around the channel length or filter length and window size L_w is satisfied.

The system model defined in this chapter is the general model for the receivers that presented in the next chapter. Some simplifications can be performed on the general system model while derivation of the receivers is performed. The details of the modifications are explained in the related sections of the next chapter.

CHAPTER 3

ANALYSIS OF CDMA DOWNLINK RECEIVERS

CDMA downlink receivers benefit from some important properties of downlink transmission. First, both desired and interfering signals are symbol-synchronous at transmitter (base station) side. Second, these symbol-synchronous signals pass through the same propagation channel. Consequently, these two properties provide that spreading sequences from an orthogonal set can be used for all users.

There is a significant amount of research work on detection and estimation of transmitted signal under different communication channels. In general, optimal decision rules and variables may contain nonlinearity. However, nonlinearity of detection or estimation results in increased computational complexity. Computational complexity can be more apparent when the system parameters grow up. In a L-path frequency-selective fading channel, optimal detection of desired data sequence can be performed by the maximum likelihood sequence detector (MLSD) [8] , with time complexity of $O(2^L)$. In a K-user flat-fading channel, computational complexity of optimal multiuser detection per user can be represented as $O(2^K/K)$ [3]. When the communication channel includes both multiuser and multipath effect, the optimal decision becomes harder to achieve with approximated complexity of $O(2^{KL})$.

The requirements of low-complexity and practical receivers have lead to the linear receivers to take more attention. The suboptimality of the linear receivers may cause performance loss in particular situations. The bottleneck for the system performance

can be sometimes receiver design parameters, and sometimes can be system design parameters or requested service requirements.

In this chapter, we analyze the different CDMA downlink receivers in different environments. Section 3.1 starts with the optimal receiver structure for single-user in the absence of multipath propagation. Introduction of this basic system model is followed by Section 3.2 that defines the conventional RAKE receiver, which makes use of path diversity under multipath channel conditions. After this section, Section 3.3 gives the structure of the linear optimal full-rank MMSE receiver. The optimal full-rank receiver is explored and investigated using some parameters. Last two sections, Section 3.4 and Section 3.5, present the suboptimal low-complexity receivers, which will be compared with full-rank MMSE receiver. The first suboptimal receiver is based on chip-level equalization. The second one adds interference suppression ability to the conventional RAKE, which is introduced in Section 3.2.

3.1. Matched Filter

In additive white Gaussian noise (AWGN) channel or flat fading environment with only one user, the linear detector known as matched filter is the optimal receiver in the sense of maximizing signal-to-noise ratio[3]. The expression in (2-1) is simplified to single user with periodic (independent of symbol) spreading code case by dropping user index k and symbol index m of spreading sequence as:

$$x[n] = a\, s[m]\, c[n \ Mod \ N] \tag{3-1}$$

The vector form of transmitted chips over one symbol period can be shown as:

$$\mathbf{x} = as\mathbf{c} \tag{3-2}$$

where a is transmitted signal amplitude, s is transmitted symbol (e.g., $s = \pm 1$ for BPSK) and $\mathbf{c}$ is the spreading code vector represented as $\mathbf{c} = [\ c[mN], c[mN+1], \ldots, c[mN+N-1]\ ]^T$. We can represent the output of the chip rate sampling of the received signal over one symbol period as:

$$\mathbf{y} = \alpha \mathbf{x} + \mathbf{w} \tag{3-3}$$

where for m th symbol $\mathbf{y} = [\ y[mN], y[mN+1], \ldots, y[mN+N-1]\ ]^T$ and $\mathbf{w}$ is similarly defined noise vector as in Section 2.3 . For flat fading case, it is assumed that fading is slow enough to consider channel coefficient α as constant during one symbol (or N chip) period.

A linear detector calculates the sign of the real part of the multiplication of received sample vector and deterministic filter vector:

$$\hat{s} = \mathrm{sgn}(\Re(\mathbf{f}^{\mathrm{H}}\mathbf{y})) \tag{3-4}$$

All positive multiples of $\alpha^*\mathbf{c}$, $\mathbf{f_{MF}} = \beta\alpha^*\mathbf{c}$, are candidates for the matched filter [3]. If the additive zero-mean noise is white Gaussian, the matched filter also minimizes the probability of error. The bit error probability for this case can be expressed in terms of the Q function[1]:

$$P_b = Q\left(\sqrt{\frac{a^2|\alpha|^2 NE_c}{N_0/2}}\right) \tag{3-5}$$

---

[1] $Q(x) = \frac{1}{\sqrt{2\pi}} \int_x^\infty \exp\left(-\frac{y^2}{2}\right) dy$

where $N_0/2$ represents noise variance. If additional synchronous users added in this single path or frequency-nonselective channel, the matched filter is not optimal in the maximum signal-to-interference-plus-noise sense. The multiuser received samples of general model of the previous chapter can be modified for single path channel as

$$\mathbf{y} = \alpha \mathbf{CAs} + \mathbf{w} \tag{3-6}$$

where $\mathbf{C}$ is $N \times K$ spreading code matrix whose kth column is $\mathbf{C_k}$. Since there is no inter chip interference caused by multipaths, $\mathbf{C_k}$ has single column.

The optimality of the matched filter can be preserved if the orthogonal signature waveforms are used for spreading process. The output of matched filter can be shown as

$$\alpha^* \mathbf{c_k}^{\mathrm{H}} \mathbf{y} = |\alpha|^2 N E_c A_k s_k + |\alpha|^2 \sum_{j \neq k} A_j s_j \rho_{jk} + n_k \tag{3-7}$$

where $\rho_{jk} = c_k^H c_j$ can be defined as correlation between kth and jth user code with real-valued codes $\rho_{kk} = c_k^H c_k = NE_c = E_b$. If the orthogonal set of codes is used, then $\rho_{jk} = 0$, $j \neq k$ and we conclude with the same result in the single user case:

$$\alpha^* \mathbf{c_k}^{\mathrm{H}} \mathbf{y} = |\alpha|^2 N E_c A_k s_k + n_k \tag{3-8}$$

The probability of error also can be calculated the same as single user case. However, if the nonorthogonal codes are used, the probability of error suffers from multiuser interference and the approximated bit-error-rate (BER) of [3] with addition of fading channel effect will be

$$P_b = Q\left(\sqrt{\frac{A_k^{\,2}|\alpha|^2 NE_c}{N_0/2 + |\alpha|^2 \sum_{j\neq k} A_j^{\,2}\rho_{jk}}}\right) \tag{3-9}$$

The expression given in (3-9) reveals that addition of equal-power user, which is usual for downlink communication in the CDMA channel, may cause significant degradation in the BER performance if the correlation properties of spreading codes are not well designed.

Under multipath propagation channel conditions, the desired signal at receiver faces interference caused by delayed versions of the transmitted multiuser signal. First part of the interference is multiple-access interference (MAI) such that orthogonality of spreading codes will be lost due to shifted copies of the signals. Second part of the total interference is interchip interference (ICI) that the desired user signal component from another resolvable path acts like nonorthogonal signal of another user with same transmitted symbol. The system model, which we have defined in Chapter 2, uses short orthogonal spreading codes, and hence the autocorrelation of desired user code is not likely to be a discrete-delta function when the delay spread is relatively large with respect to symbol period. In order to compensate ICI and MAI in such a case, spreading factor must be chosen sufficiently larger than the delay spread in chips.

Both delay spread and distribution of channel coefficients affect the performance of matched filter. Frequency-selective CDMA channels require the receivers that can perform better than the matched filter that only tries to match spreading code of desired user. The receivers having better performance under multiuser and multipath communication channel are investigated in the following sections.

3.2. Conventional RAKE Receiver

In a multipath fading propagation channel, the optimum way of path diversity combining is using a demodulator structure known as RAKE receiver [1], [2]. The RAKE receiver can be configured as two different structures, which are shown in Figure 3-1 and Figure 3-2. Both configurations consist of L parallel branches to combine all the desired signal energy from L multipaths. Each branch is called a "finger" of the RAKE receiver.

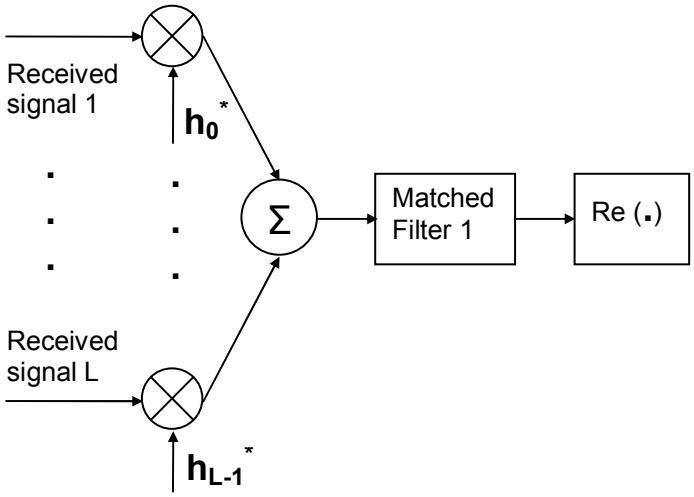

Figure 3-1: Block diagram of Rake receiver with predetection combining

The optimal coherent matched filtering or spreading waveform correlation is a linear operation on the received sample vector. Consequently, both predetection combining, which is shown in Figure 3-1; and postdetection combining, which is shown in

Figure 3-2, give the same result for symbol detection if finger coefficients of two configurations are the same.

The filter of single-user optimal receiver in the frequency-nonselective channel, only matches the spreading code of desired user and phase of the single channel tap. Maximal ratio combining (MRC) technique is the way of matching to all the channel taps to benefit from path diversity. If MRC is applied in the selection of finger coefficients, the conventional RAKE receiver requires that the propagation channel coefficients are known or estimated. In this work, we assume that the conventional RAKE receiver has the perfect knowledge of the propagation channel. Since we have exact channel coefficients we can use MRC in performance analysis, and hence channel estimation error has no effect on the performance. MRC technique is shown to be optimal in [2] if the interference-plus-noise signals in all the branches are uncorrelated.

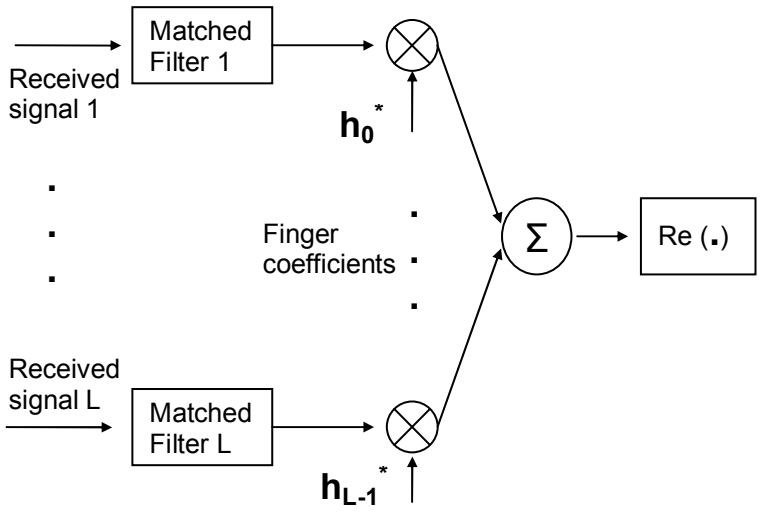

Figure 3-2: Block diagram of Rake receiver with postdetection combining

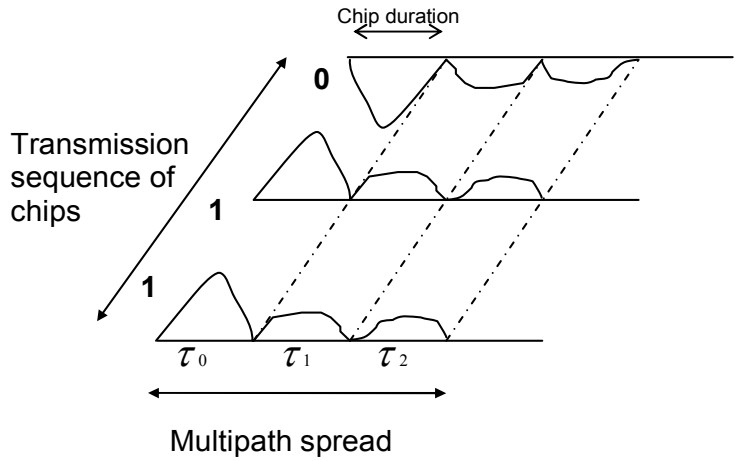

Figure 3-3: Received chip samples with chip-rate multipath components

Other combining methods such as selection combining (SC), equal-gain combining (EGC) are compared with MRC in [2], [4] and [6]. It is shown that MRC performs better than the other two methods. Also, increasing number of finger does not always produce positive effect on the performance of the receiver. If desired signal component in that branch is relatively weak, addition of fingers at required positions may not improve the performance of the EGC, but degrades because of additional strong unwanted signal. On the other hand, since MRC tries to match the channel, MRC does not introduce additional noise. In the next subsection, postdetection MRC RAKE receiver is examined. The performance of the RAKE receiver in the next chapter is evaluated using this configuration.

3.2.1. Postdetection MRC RAKE Receiver

Conventional RAKE receiver has already been used in current CDMA systems [9]. RAKE receiver can take advantage of MRC technique if channel coefficients are known or accurately estimated. For the postdetection MRC RAKE receiver, which is

shown in Figure 3-2, multipath spreading caused by delays located at chip rate is illustrated in Figure 3-3 .

As shown in Figure 3-3, there are three resolvable multipath components in this example that resolvability is defined in Section 2.2. Assuming that receiver has single antenna, Figure 3-2 can be reconfigured as depicted in Figure 3-4.

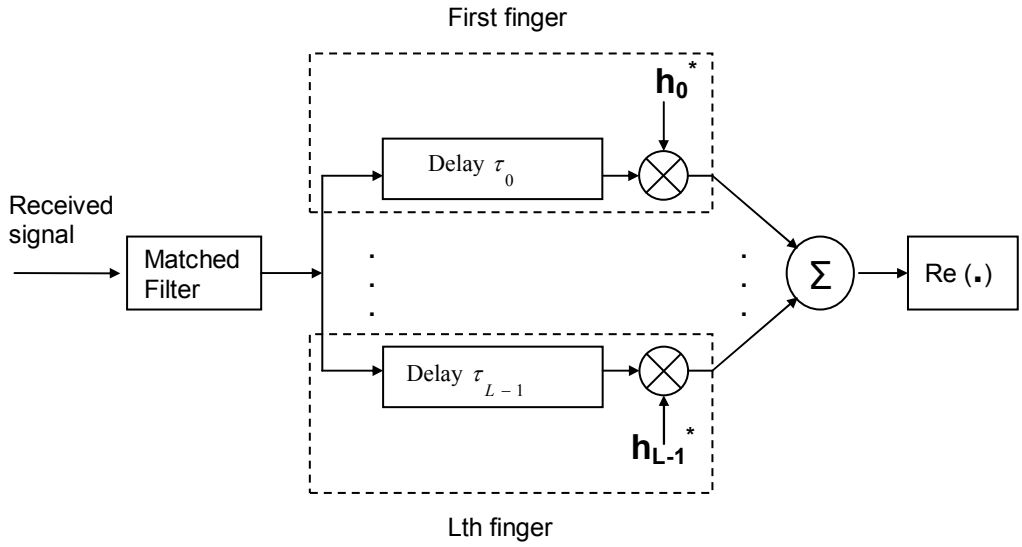

Figure 3-4: RAKE receiver structure with single matched filter and with L fingers

The RAKE receiver structure can be represented in a vector form using derivation of previous chapter. The output of the matched filter can be expressed such that chip sampled received vector $\mathbf{y}$ is multiplied by the matrix $\mathbf{U}_k$ whose rows contain the code vector of the desired user.

$$\mathbf{z} = \mathbf{U}_k \mathbf{y} \tag{3-10}$$

where $\mathbf{U}_k$ is $L \times (N + L - 1)$ matrix, which can be defined as:

$$\mathbf{U}_k = \begin{bmatrix} c_k[0] & c_k[1] & \cdots & \cdots & \cdots & c_k[N-1] & 0 & \cdots & 0 \\ 0 & c_k[0] & \cdots & \cdots & \cdots & c_k[N-2] & c_k[N-1] & \vdots & \vdots \\ \vdots & \vdots & \ddots & \vdots & \vdots & \vdots & \vdots & \vdots & 0 \\ 0 & \cdots & 0 & c_k[0] & \cdots & c_k[N-L] & c_k[N-L-1] & \cdots & c_k[N-1] \end{bmatrix}_{L \times (N+L-1)} \tag{3-11}$$

The decision variable for user data is obtained as multiplication of the output of the matched filter by another matched filter. The second filter is matched to the channel. The coefficients of the MRC RAKE fingers are obtained by the tap weights of the second matched filter. At the end of the receiver, the estimated user data bit can be calculated as:

$$\bar{s} = \text{sgn}(\Re(\mathbf{h}^{\mathbf{H}} \mathbf{z})) \tag{3-12}$$

The signal-to-interference-plus-noise ratio (SINR) and the bit error probability (BEP) of conventional MRC RAKE receiver is calculated in [2] under the channel condition that independent L paths have identical Rayleigh distribution with $E\left[|h_i|^2\right] = |\alpha|^2$, $0 \le i \le L-1$. SINR calculation is performed assuming interference-plus-noise as white zero-mean Gaussian noise with variance of σ_u^2. Since conventional RAKE receiver treats the total interference as white Gaussian noise, signal-to-noise ratio (SNR) given in reference [2] can expressed for the model of this section as

$$SNR_{RAKE} = \frac{NE_c \mathbf{h}^H \mathbf{h}}{2\sigma_u^2} = \frac{E_b \mathbf{h}^H \mathbf{h}}{2\sigma_u^2} \tag{3-13}$$

and its average value is

$$\overline{SNR}_{RAKE} = \frac{E_b E\left[\mathbf{h}\mathbf{h}^H\right]}{2\sigma_u^2} = \frac{E_b L|\alpha|^2}{2\sigma_u^2} = L\bar{\gamma} \tag{3-14}$$

where $\bar{\gamma}$ is average SNR per branch The BEP of conventional RAKE given in [2] becomes for this case

$$P_b(L) = p^L \sum_{i=0}^{L-1} \binom{L+i-1}{i} (1-p)^i \le \binom{2L-1}{L} p^L \tag{3-15}$$

where

$$p = \frac{1}{2}\left(1 - \sqrt{\frac{\bar{\gamma}}{1+\bar{\gamma}}}\right) \tag{3-16}$$

3.2.2. Other RAKE Receivers

The multipath channel, which is shown in Figure 3-3, can be easily tracked and estimated since the channel delays are spaced by chip period and fixed in time. The propagation channel may not be so tractable and predictable if the channel has a sparse impulse response. A receiver estimating the desired symbol as a nonlinear function of the received chip-rate samples for sparse channels without multi-access interference is given in [10].

A general finger placement method for 3-ray Rayleigh channel model is used in [11]. It searches the continuous interval that covers a few times larger than delay spread for asymptotical analysis. A practical version of finger placement method that uses chip periodically spaced fingers is given in [19]. However, it treats the total interference as colored Gaussian noise and uses maximum-likelihood formulation to calculate finger coefficients.

In the following three sections, we will analyze the linear minimum mean square error (MMSE) based receivers that can operate under multipath and multiuser channel conditions. These are full-rank LMMSE, chip-level LMMSE and interference-suppressing (MMSE based) RAKE receiver. These receivers differs from the previously mentioned receivers in that the new MMSE based method does not necessarily assume uncorrelated branches, approximation on interference structure and fixed number of fingers.

3.3. Full-Rank LMMSE Receiver

The conventional RAKE receiver has a performance limited by the number of active users. The performance of the RAKE receiver may be acceptable in the communication channels where the ratio of number of active users to spreading factor is small (e.g. $K / N \approx 0.2$) [18]. Since the conventional RAKE receiver does not construct a powerful mechanism for multi-access interference (MAI) of large number of users, interference-suppressing techniques are required for higher performance of the receiver.

Interference suppression and noise level reduction can be achieved at the same time by the application of the mean-square error (MSE) cost criterion. The MSE cost function of single user estimation is given by (3-17).

$$C(s_k, \hat{s}_k) = E\left[\left| s_k - \hat{s}_k \right|^2\right] \tag{3-17}$$

In the classical estimation theory, the aim of the estimation process is to minimize the risk or cost function [17]. Bayes' least-squares (BLS) estimator that minimizes the MSE cost function is the optimal method if the complete statistical characterization between received chip sample vector and desired user's transmitted

signal is perfectly known. The compact expression of the BLS estimator can be shown as

$$\hat{s}_{k,BLS}(\mathbf{y}) = E[s_k \mid \mathbf{y} = y] \tag{3-18}$$

The Bayes' least-squares estimator can be considered impractical that requires full knowledge of marginal and conditional density functions and computationally complex operations of nonlinear functions [5]. In the case of multiuser and multipath environment, acquiring the required information is more difficult.

The partial statistical knowledge of multiuser and multipath condition and requirement of low-complexity practical structures results in a development of suboptimal receivers. In this thesis work, the form of the suboptimal receivers is selected as linear function of the received chip sample vector $\mathbf{y}$.

The vector model $\mathbf{y}$ of the received data, which is built on previous section, is the starting point of the derivation of the full-rank, i.e. symbol-level, linear minimum mean square error (LMMSE) receiver. This chip-rate sample vector model of the received data is widely accepted for different type of CDMA multiuser receivers such as in [7] for symbol-level LMMSE under single-path condition, additionally, the structures given in [12], [13], and [14] for the receivers of next sections. The linear MMSE estimate can be simply depicted by assuming real-valued user symbol and real-valued vectors

$$\mathbf{g}_{k,symbol} = \arg\min_{g} E\left[\left|s_k - (\mathbf{g}^T\mathbf{y})\right|^2\right] \tag{3-19}$$

$$\hat{s}_k = \mathbf{g}_{k,symbol}^T\mathbf{y} \tag{3-20}$$

where $\mathbf{g}_{k,symbol}$ is the weight vector of the linear MMSE receiver with $\mathbf{g}_{k,symbol} = \left[g_{k,0}\ g_{k,1} \cdots g_{k,L_w-1}\right]^T$. The size of the vector $\mathbf{g}_{k,symbol}$ and $\mathbf{y}$ is $L_w \times 1$ and determined by the number of chips per bit N and the maximum order of the channel impulse response in chips $L-1$. Observation window size L_w should satisfy $L_w \geq N + L - 1$ in order to achieve full-rank approximation. The signal model that is assumed real-valued for simplicity can be generalized to complex-valued signal model with some modification.

Orthogonal Projection Theorem [5], can be used to acquire normal equations that determine the optimal coefficients of vector $\mathbf{g}$. The estimate $\hat{s}_k$ must satisfy the orthogonality condition

$$\left\langle s_k - \hat{s}_k\ , y_n \right\rangle = 0,\ \ n = 0,1,\ldots,L_w - 1 \tag{3-21}$$

where y_n is the $(n+1)$th element of $\mathbf{y}$. Using orthogonality condition,

$$\left\langle s_k , y_n \right\rangle = \left\langle \mathbf{g}_{k,symbol}{}^T \mathbf{y}, y_n \right\rangle = \sum_{i=0}^{L_W-1} g_{k,i} \left\langle y_i , y_n \right\rangle,\ \ n = 0,1,\ldots,L_w - 1 \tag{3-22}$$

L_w normal equations can be collected into vector and matrix form. By taking expectations of matrix form of the equations, we get the resultant equation as

$$\mathbf{R}_{\mathbf{yy}} \mathbf{g}_{k,symbol} = \mathbf{r}_{sy} \tag{3-23}$$

where the autocorrelation of chip sampled received signal is

$$\mathbf{R}_{\mathbf{yy}} = E\left[\mathbf{y}\mathbf{y}^{\mathrm{T}}\right] \tag{3-24}$$

and crosscorrelation of desired signal and received signal is

$$\mathbf{r}_{sy} = E[\mathrm{s_k}\mathbf{y}] \tag{3-25}$$

These equations can also be derived by using Wiener-Hopf method [5]. Collecting L_w Wiener-Hopf equations into vector form, again Equation (3-23) can be obtained. If the matrix $\mathbf{R}_{\mathrm{yy}}$ is positive definite and hence invertible, the optimal weight vector can be expressed as

$$\mathbf{g}_{k,symbol} = \mathbf{R}_{\mathrm{yy}}^{-1}\mathbf{r}_{sy} \tag{3-26}$$

When $\mathbf{R}_{\mathrm{yy}}$ is singular and not invertible, any solution of (3-23) will be optimal. The solution of (3-26) seems to be completely depending on observation window of estimated symbol. In order to obtain a more apparent representation of the weight vector of the linear full-rank MMSE receiver, the received chip sample vector can be decomposed into elements given in Table 3-1 .

Hereafter to simplify calculations, transmitter and channel parameters are modified into forms that are more suitable. The diagonal amplitude matrix $\mathbf{A}$ whose diagonal entries contain users' signal amplitude can be taken as unity identity matrix $\mathbf{I}$ assuming that transmit power of all the users are equal and not amplified. The new expression of the required data will become

$$\mathbf{y} = \mathbf{HCs} + \mathbf{w} \tag{3-27}$$

where channel model of (2-5) is simplified to

$$h(t) = \sum_{l=0}^{L-1} h_l\,\delta(t - lT_c) \tag{3-28}$$

such that two adjacent paths are separated by one chip-period. First path synchronization is applied so that h_0 is the coefficient of the first received path. Although channel model has an impulse response with order of $L-1$, the channel coefficients can be zero except for h_0 and h_{L-1}.

Table 3-1: Elements of full-rank MMSE receiver.

Representation	Description	Size	Statistical Knowledge
H	Channel Convolution Matrix	$L_w \times (L_w + L - 1)$	Deterministic Complex-valued
C	Multiuser Code Matrix	$(L_w + L - 1) \times (3K)$	Deterministic Real-valued
s	Multiuser Symbol Vector	$3K \times 1$	Stochastic Real-valued
w	Additive Gaussian Noise	$L_w \times 1$	Stochastic Complex-valued

Once the transmission scenario of the multiuser signal is completed, the reception of the signal can be revised in order to simplify the receiver analysis. At the receiver frontend before chip-level sampling, a series of continuous-time processing is applied. Initially a downconversion process is performed and then baseband pulse shaping matched filtering is constructed prior to chip-level sampling [8]. This processing chain reshapes the variables such that the real-valued additive white Gaussian noise becomes complex-valued circularly symmetric colored Gaussian noise [2]. However, it is acceptable that colorization of the noise can be ignored if

spreading is wide enough or $1/T_c \to \infty$ [2]. Another convention for white Gaussian assumption is that initial noise can be whitened by an orthonormal linear transformation [7].

The calculation of the optimal weight vector of the linear full-rank MMSE receiver can be achieved with the help of the above statements of transmission and reception. We can expand (3-24) and (3-25) as follows:

$$\begin{aligned}\mathbf{R}_{\mathbf{yy}} &= E[\mathbf{y}\mathbf{y}^{\mathrm{H}}] \\ &= E[(\mathbf{HCs}+\mathbf{w})(\mathbf{HCs}+\mathbf{w})^{\mathrm{H}}] \\ &= \mathbf{HCR}_{\mathbf{SS}}\mathbf{C}^{\mathrm{H}}\mathbf{H}^{\mathrm{H}} + \mathbf{R}_{\mathbf{ww}}\end{aligned} \tag{3-29}$$

where $\mathbf{R}_{\mathbf{SS}} = E[\mathbf{s}\mathbf{s}^{\mathrm{H}}]$, $\mathbf{R}_{\mathbf{ww}} = E[\mathbf{w}\mathbf{w}^{\mathrm{H}}]$ and it is assumed that symbols are independent with respect to the additive noise such that $\mathbf{R}_{\mathbf{sw}} = E[\mathbf{s}\mathbf{w}^{\mathrm{H}}] = 0$. The definition of the **s** is given in (2-14).

The same operations can be applied to crosscorrelation vector with:

$$\begin{aligned}\mathbf{r}_{sy} &= E[\mathrm{s}_{\mathrm{k}}\mathbf{y}] \\ &= E[s_k(\mathbf{HCs}+\mathbf{w})] \\ &= \mathbf{HCe}_{3(k-1)+2}\end{aligned} \tag{3-30}$$

where $\mathbf{e}_{3(k-1)+2}$ is the $3K \times 1$ vector that entries are all zeros except for one in the $(3(k-1)+2)$th row. Consequently, the weight vector is formed as

$$\mathbf{g}_{k,symbol} = \mathbf{R}_{\mathbf{yy}}^{-1}\,\mathbf{r}_{sy}$$

$$\mathbf{g}_{k,symbol} = (\mathbf{HCR}_{\mathbf{SS}}\mathbf{C}^{\mathrm{H}}\mathbf{H}^{\mathrm{H}} + \mathbf{R}_{\mathbf{ww}})^{-1}\,\mathbf{HCe}_{3(k-1)+2} \tag{3-31}$$

The correlation matrix of the zero-mean noise can be taken as diagonal matrix $\mathbf{R}_{\mathbf{ww}} = N_0\mathbf{I}$ because of white assumption.

There can be two more assumptions on transmission of each user symbol stream. Firstly, symbols of each user yield a white stream that means independent in time with respect to itself. Secondly, the symbols of each user are independent of symbol stream of other users. The stated independent assumptions produce $\mathbf{R}_{\mathbf{SS}} = \mathbf{I}$ and the Equation (3-31) is reduced to

$$\mathbf{g}_{k,symbol} = (\mathbf{HCC}^{\mathrm{H}}\mathbf{H}^{\mathrm{H}} + N_0\mathbf{I})^{-1}\,\mathbf{HCe}_{3(k-1)+2} \tag{3-32}$$

From the Equation (3-32) several implications can be obtained:

All multipath components are directly included in the observation window of the full-rank solution provided that $L_w \geq N + L - 1$ is satisfied. Thus, positive effect of multipath diversity can be seen from the representation of effective channel of desired user $\mathbf{HCe}_{3(k-1)+2}$.

Although the solution is optimal in the linear MMSE sense, it is related to an observation window that has particular position in time. In other words, a delay can be applied for observation window and further optimization can be made by searching for starting point of observation window and hence multiuser code matrix whose size is $(L_w + L - 1) \times 3K$. The position of the fixed-length observation window

in time can be initialized by fixing the first chip sample or last chip sample. If we reference the last received chip sample as $y[mN+N-1]$, the observation window can be initialized in a similar way of [13] and [14]. The initial observation window generates the following representations: The received chip sample vector is formed stacking L_w chip samples starting with the sample $y[mN+N-L_w]$ until last chip sample of the desired symbol $y[mN+N-1]$ is obtained.

$$\begin{aligned}\mathbf{y} = [\, & y[mN+N-1], y[mN+N-2], \ldots, y[mN], y[mN-1], \ldots, \\ & y[mN+N-(L_w-1)], y[mN+N-L_w]]^T\end{aligned} \tag{3-33}$$

The required code matrix of k th user will be,

$$\mathbf{C_k} = \begin{bmatrix} c_k[N-(L_w-N+L_h)] & 0 & 0 \\ c_k[N-(L_w-N+L_h)+1] & \vdots & \vdots \\ c_k[N-(L_w-N+L_h)+2] & & \\ \vdots & & \\ c_k[N-2] & & \\ c_k[N-1] & 0 & 0 \\ 0 & c_k[0] & 0 \\ \vdots & c_k[1] & \vdots \\ \vdots & \vdots & \\ & & \\ & & \\ & & \\ & c_k[N-2] & \\ 0 & c_k[N-1] & 0 \end{bmatrix} \tag{3-34}$$

where the order of the propagation channel is represented as L_h, with the equality of $L_h = L-1$. The Equation (3-33) says that the observation window covers two symbols such that the last $L_w - N$ chips of previous symbol are included in addition

to N chips of desired symbol. Initially, few chips related to the next symbols are not required.

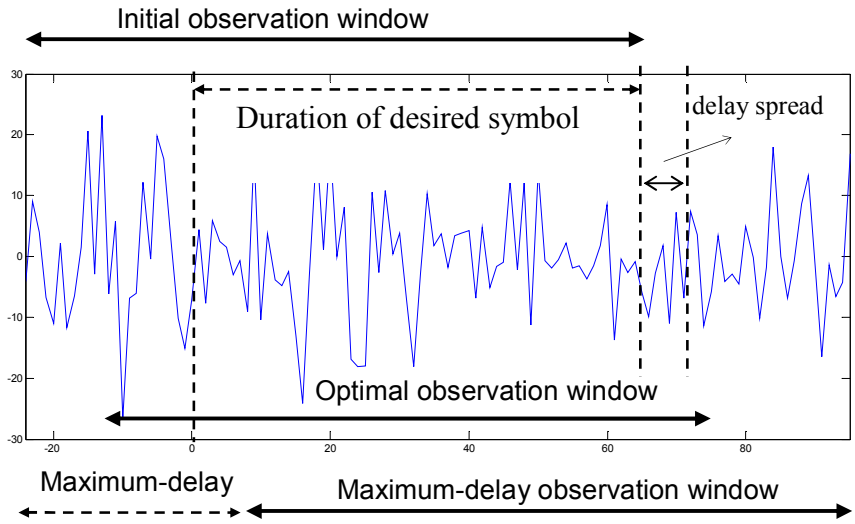

Figure 3-5: Representation of observation window and maximum delay

The analytical explanation of the selection of initial observation window can be completed considering Figure 3-5 as follows: Assume that the desired symbol is $s_1[0]$ and the transmitted chips related to $s_1[0]$ is first received at $y[0]$. We can express $y[0]$ as linear combination of transmitted chip samples and noise $y[0] = \sum_{l=0}^{L_h} h_l x[0-l] + w[0]$. To eliminate effect of interference (ISI, ICI and MAI) we need scaled copies of interfering chips, and hence available maximum number of

weights are accommodated for previous chips at the initial window such that $\hat{s}_k[0] = \mathbf{g}_{k,symbol}^T \mathbf{y} = \sum_{j=0}^{L_w-1} g_{k,j}\, y[j + N - L_w]$.

The multipath components of desired symbol are directly included, however initially not covered completely as shown in Figure 3-5. Since the first chip of desired symbol can be recovered at $y[L_h]$, the maximum delay that can be applied to fixed length window is determined by delay spread and hence it will be $((L_w - N) + L_h)$. Eventually, an optimal window should be searched such that MMSE related to the observation window, which is delayed by D chip, is also minimum of all the possible $(L_w + L_h - N + 1)$ delayed versions. The required MMSE expression can be obtained by direct substitution of (3-20) into (3-17) and using (3-21),

$$MMSE_{symbol} = 1 - \mathbf{g}_{k,symbol}^H \mathbf{r}_{sy} \tag{3-35}$$

Substituting (3-30) and (3-31), we can conclude that

$$MMSE_{symbol} = 1 - \mathbf{e}^H{}_{3(k-1)+2} \mathbf{C}^{\mathrm{H}} \mathbf{H}^{\mathrm{H}} (\mathbf{H}\mathbf{C}\mathbf{C}^{\mathrm{H}}\mathbf{H}^{\mathrm{H}} + N_0\mathbf{I})^{-1} \mathbf{H}\mathbf{C}\mathbf{e}_{3(k-1)+2} \tag{3-36}$$

The required received sample vector for D-chip-delayed solution will become

$$\begin{aligned} \mathbf{y} = [\, & y[mN + N - L_w + D], y[mN + N - (L_w - 1) + D], \ldots, \\ & y[mN - 1], y[mN], y[mN + 1], \ldots, y[mN + N - 1 + D]]^T \end{aligned} \tag{3-37}$$

Also, the multiuser code matrix $\mathbf{C}$ must be slightly modified shifting the $\mathbf{C}$ by D rows below. The delay of observation window causes that the chips related to the

next symbols must be taken into account. Accordingly, the required code matrix of k th user can be expressed as

$$\mathbf{C_k} = \begin{bmatrix} c_k[N-(L_r+L_h)+D] & 0 & 0 \\ c_k[N-(L_r+L_h)+1+D] & \vdots & \vdots \\ \vdots & & \\ c_k[N-2] & & \\ c_k[N-1] & 0 & 0 \\ & c_k[0] & 0 \\ 0 & c_k[1] & \vdots \\ \vdots & \vdots & \\ \vdots & c_k[N-2] & \\ & c_k[N-1] & 0 \\ & 0 & c_k[0] \\ & \vdots & \vdots \\ 0 & 0 & c_k[D-1] \end{bmatrix} \tag{3-38}$$

where the number of extra taps L_r is substituted for $(L_w - N)$. The code matrix of all the users can be formed in the same way. Consequently, the multiuser code matrix can be constructed by concatenation of individuals' matrices. Since the effect of delay cannot be represented in (3-32) and (3-36) explicitly, an exhaustive search can be applied as a conventional method. Since the optimal delay depends on both channel parameters and number of active users because of multiuser code matrix, it seems that an exhaustive search is not practical. To reduce the complexity of delay search for full-rank LMMSE, we will make use of the result that will be obtained in the solution of chip-level LMMSE. The details of delay search and its significance on performance will be explained in the next chapter.

After solving the delay search problem, the major drawback of the full-rank MMSE solution is the computational complexity of the construction of $L_w \times L_w$ correlation matrix $\mathbf{R}_{\mathbf{yy}}$ and its inverse $\mathbf{R}^{-1}{}_{\mathbf{yy}}$. When the channel parameters and code vectors of

all users are known as in the case of simulations of next chapter, multiplication operations of $(\mathbf{HCC}^{\mathrm{H}}\mathbf{H}^{\mathrm{H}} + \mathbf{R}_{\mathbf{ww}})$ and inversion of the $L_w \times L_w$ matrix still require much more processing power with the increasing number of users and length of observation window. Some simplifications can be performed on the full-rank LMMSE receiver to handle these difficulties. The two methods that reduce the number of calculations can be explained as follows:

For the particular situation that the system is fully loaded as $K=N$ (number of users is equal to the spreading gain), the matrix product $\mathbf{CC}^{\mathrm{H}}$, which shows the correlation of codes, has a special structure. Each row of $\mathbf{C}$, accordingly each column of $\mathbf{C}^{\mathrm{H}}$, contains the complete set of concerned code sequence that is contained in the related row or column of $N\times N$ Hadamard matrix $\mathbf{M}_N$. In this case, the size of multiuser code matrix becomes ($L_w\times 3N$) that the rows of $\mathbf{C}$ can be constructed from $\mathbf{M}_N$. as follows: Interested orthogonal rows $\mathbf{M}_N$. are upsampled by 3, padding two zeros after one chip, and inserted into first $(L_r + L_h - D)$ rows of $\mathbf{C}$. Next N rows of $\mathbf{C}$ are constructed inserting the interested rows of $\mathbf{M}_N$. after shifting to the right by one. The last D rows of $\mathbf{C}$ are similarly constructed from related rows of $\mathbf{M}_N$. shifting to the right by two instead of one. This construction method reveals the fact that the all rows of $\mathbf{C}$ are orthogonal because they are upsampled and shifted versions of those of $\mathbf{M}_N$. Note that in this particular situation, the combination of upsampling and the linearly shifting to the right does not destroy the orthogonality of codes. Consequently, we can obtain the simplified product of code matrices as $\mathbf{CC}^{\mathrm{H}} = K\mathbf{I} = N\mathbf{I}$. This interesting result can also be used when $K\leq N$ in the expanse of lowered performance while K goes from N to 1. The simplification on correlation of code matrix, however, does not change the complexity of inversion of $L_w \times L_w$ matrix.

For the particular situation that the system is moderately loaded as $3K\leq N$, the complexity of inversion of $L_w \times L_w$ matrix can be reduced by using another

representation of weight vector in terms of interested matrices. In this case, to make calculation of weight vector simpler, we can use a form of matrix inversion lemma [20] as

$$(\mathbf{P}+\mathbf{UQV})^{-1}=\mathbf{P}^{-1}-\mathbf{P}^{-1}\mathbf{U}(\mathbf{Q}^{-1}+\mathbf{VP}^{-1}\mathbf{U})^{-1}\mathbf{VP}^{-1} \tag{3-39}$$

where **P** and **Q** must be invertible. After matching the matrices used in (3-32) and (3-39) as $\mathbf{P}=N_0\mathbf{I}$, $\mathbf{U}=\mathbf{HC}$, $\mathbf{V}=\mathbf{C}^{\mathrm{H}}\mathbf{H}^{\mathrm{H}}$ and $\mathbf{Q}=\mathbf{I}$ we can get

$$\mathbf{g}_{k,symbol}=\mathbf{HC}(\mathbf{C}^{\mathrm{H}}\mathbf{H}^{\mathrm{H}}\mathbf{HC}+N_0\mathbf{I})^{-1}\mathbf{e}_{3(k-1)+2} \tag{3-40}$$

This new representation of weight vector shows that the inverted matrix has a smaller size, which is $3K\times 3K$, than the inverted matrix given in (3-32), whose size is $N\times N$.

The estimated value of desired user's symbol $\hat{s}_k$ can be converted to its transmitted binary value as

$$\bar{s}_k=\mathrm{sgn}(\Re(\hat{s}_k)) \tag{3-41}$$

The performance of the full-rank LMMSE receiver can be evaluated by calculating the signal-to-interference-plus-noise ratio (SINR) and bit error probability (BEP). The SINR of the optimal receiver can be expressed in terms of MMSE as

$$SINR_{symbol}=(MMSE_{symbol})^{-1}-1 \tag{3-42}$$

Since $\hat{s}_k$ is complex-valued and only real part of $\hat{s}_k$ is considered for decision of s_k, the SINR of BPSK can be written as $SINR_{BPSK}=2SINR_{symbol}$ assuming that

imaginary part of interference has half of the complex value of interference. Finally, assuming interference has a Gaussian distribution, we can write the BEP of full-rank LMMSE with BPSK as

$$BEP_{symbol} = Q(\sqrt{SINR_{BPSK}}) \tag{3-43}$$

The approximate average BEP of the receiver under L-path Rayleigh fading channel with identical channel taps can be calculated from the BEP expression given in (3-15) and (3-16) using the approximation $L\bar{\gamma} \approx SINR_{symbol} = SINR_{BPSK}/2$. This approximate BEP holds for any linear receiver with Gaussian interference assumption and valid for the following receivers.

3.4. Chip-level LMMSE Equalizer

As illustrated in Figure 3-3, the multipath propagation channel causes the pulses to become wider. This broadening of the pulses results in interchip interference (ICI). When the symbols are transmitted as a continuous stream, spreading effect of the channel also causes symbols to interfere with previous and next few symbols. The performance degradation of both intersymbol interference (ISI) and ICI can be significant unless the channel distortion is compensated. The technique used for the elimination of the phase and amplitude distortion of the channel is called equalization.

When the equalizer is constrained to reduce interference (ISI and ICI) completely, it is called zero-forcing (ZF) equalizer. Since the equalization of the channel also amplifies the additive noise, a solution should be generated between minimizing interference and minimizing the noise at the output.

In this section, we examine the linear MMSE equalizer at chip-rate as the solution of interference and noise minimization at the same time. The equalization technique can also be applied in a nonlinear method such as decision-feedback equalizer (DFE) [8]. Due to its feedback structure, DFE has a potential for error propagation that may cause performance loss.

The chip-rate linear MMSE equalizers that are developed by [13], [15], [16], and [18] constitute a general framework for this section. The common main property of these receivers is that equalization is used to restore the transmitted multiuser chip sequence. The equalization is performed at chip-level by applying well-known linear MSE cost function. We focus on the analysis of the receiver given in [13] because of the reasons that are explained in the following part of this section.

At this point, we can build up chip-rate linear MMSE equalizer with the help of general received signal model of Chapter 2. The received signal

$$\mathbf{y} = \mathbf{HCs} + \mathbf{w}$$

can be used to minimize the MSE for nth chip $\min_{g} E\left[\left| \mathbf{g}^{H} (\mathbf{Hx}[n] + \mathbf{w}) - x[n] \right|^{2} \right]$ with the following statements, which are mostly differ from [13]:

- The derivation of the chip-level LMMSE starts with our general assumption that spreading sequence of all active users and channel parameters are known.

- A single receiver antenna is used throughout this work. However, extension of the signal model for the increasing number of the antennas can be realized by appending the additional signals to the signals from the first antenna.

- Periodic and deterministic orthogonal codes of length N (e.g. Walsh-Hadamard codes) are used for spreading process. Before or after this coding, additional spreading code such as scrambling short or long codes are not used.

- Since the effective channel seen at the output of the equalizer is the convolution of the multipath propagation channel and equalizer whose order is L_g or number of weights is (L_g+1), the total length of the effective channel will be (L_g+L_h+1). The length of multiuser transmitted chip sequence vector $\mathbf{x}$ becomes (L_g+L_h+1) and length of received vector $\mathbf{y}$ becomes $L_w=(L_g+1)$.

The initial case to be considered is that the channel is equalized such that the effective channel of order (L_g+L_h) will be almost a discrete delta function at zero time reference. Before starting derivation of the receiver, the detailed structure of elements that compose the received signal can be expressed as follows:

The convolution matrix of the channel can be always formed as below regardless of symbol or chip index.

$$\mathbf{H}=\begin{bmatrix} h_{L-1} & h_{L-2} & \cdots & h_0 & 0 & \cdots & 0 & 0 & \cdots & 0 & 0 \\ 0 & h_{L-1} & \cdots & h_1 & h_0 & \cdots & 0 & 0 & \cdots & 0 & 0 \\ \vdots & \vdots & & \vdots & \vdots & & \vdots & \vdots & & \vdots & \vdots \\ \vdots & \vdots & & \vdots & \vdots & & \vdots & \vdots & & \vdots & \vdots \\ 0 & 0 & \cdots & 0 & 0 & \cdots & h_{L-1} & h_{L-2} & \cdots & h_0 & 0 \\ 0 & 0 & \cdots & 0 & 0 & \cdots & 0 & h_{L-1} & \cdots & h_1 & h_0 \end{bmatrix}_{L_w\times(L_w+L-1)}$$

The multiuser code matrix will be $\mathbf{C}=[\mathbf{C_1},\mathbf{C_2},\ldots,\mathbf{C_K}]$. Provided that $(L_g+L_h+1)\le N$, for $0\le n(\bmod N)\le(L_g+L_h-1)$ the kth user code matrix can be formed as

$$\mathbf{C_k} = \begin{bmatrix} c_k\left[N-(L_g+L_h)+n(\text{mod}\,N)\right] & 0 & 0 \\ c_k\left[N-(L_g+L_h-1)+n(\text{mod}\,N)\right] & \vdots & \vdots \\ \vdots & & \\ c_k\left[N-1\right] & 0 & 0 \\ 0 & c_k\left[0\right] & 0 \\ \vdots & \vdots & \vdots \\ 0 & c_k\left[n(\text{mod}\,N)\right] & 0 \end{bmatrix} \tag{3-44}$$

If the desired chip has index such that $(L_g + L_h) \le n\,(\text{mod}\,N) \le N-1$, $\mathbf{C_k}$ becomes

$$\mathbf{C_k} = \begin{bmatrix} 0 & c_k\left[n(\text{mod}\,N)-(L_g+L_h)\right] & 0 \\ \vdots & \vdots & \vdots \\ 0 & c_k\left[n(\text{mod}\,N)\right] & 0 \end{bmatrix} \tag{3-45}$$

The representation of transmitted symbols will be again

$$\mathbf{s} = \left[\mathbf{s_1}, \mathbf{s_2}, \ldots, \mathbf{s_K}\right]^{\mathbf{T}}$$

where

$$\mathbf{s_1} = \left[\ s_1[m-1], s_1[m], s_1[m+1]\ \right]^T$$

This initial window of equalization of the channel also causes the loss of available energy from multipath. This can be shown in (3-44) such that the second column of $\mathbf{C_k}$ contains only desired chip, on the contrary, in the RAKE receiver it contains the first L_h spreading codes related to the desired chip. Hence, the MMSE optimization procedure of chip-level LMMSE receiver can be stated as follows:

Since the MMSE solution also tries to minimize output noise level, the best effective channel that minimizes MMSE must be searched for a delayed version. Hence

observation window must be shifted by a delay of D. The MSE cost function for D-chip delay can be modified as

$$\min_{g} E\left[\left| \mathbf{g}^{H}(\mathbf{Hx}[n]+\mathbf{w}) - x[n-D] \right|^{2} \right]$$

or equivalently,

$$\min_{g} E\left[\left| \mathbf{g}^{H}(\mathbf{Hx}[n]+\mathbf{w}) - \mathbf{e}_{\overline{D}}^{T}\mathbf{x}[n] \right|^{2} \right] \tag{3-46}$$

where we use the simplified representation of $\overline{D} = L_w + L_h - D$,and $\mathbf{e}_j$ is the same as previously defined vector for full-rank MMSE.

Since the equalizer is an FIR filter with order of L_g, the effective channel may contain sidelobes that it has nonzero weights except for $\overline{D}$ th weight. These unwanted signals cause the best delay to vary for each channel realization. Different values of L_g are used for performance analysis of next chapter such that positive effect of the additional weights on BER performance will be shown in simulation results.

Once the constraints are determined, the chip-level LMMSE can be derived in the same way that we have used for symbol-level LMMSE with some differences. The parameters that differ from full-rank case are shorter observation window and desired signal, which is chip instead of symbol. Using Wiener-Hopf solution to (3-46) with D-chip delay introduced observation window, the weight vector can be obtained as

$$\mathbf{g}_{chip} = \mathbf{R}_{\mathbf{yy}}^{-1}\mathbf{r}_{x\mathbf{y}} \tag{3-47}$$

The required correlation matrix and crosscorrelation vector can be expressed as

$$\mathbf{R}_{\mathbf{yy}} = E\left[\mathbf{y}\mathbf{y}^{H}\right] = \mathbf{HCR}_{\mathbf{SS}}\mathbf{C}^{\mathrm{H}}\mathbf{H}^{\mathrm{H}} + \mathbf{R}_{\mathbf{ww}}$$

$$= \mathbf{HCC}^{\mathrm{H}}\mathbf{H}^{\mathrm{H}} + N_0\mathbf{I} \tag{3-48}$$

$$\mathbf{r}_{x\mathbf{y}} = E[(\mathbf{Hx}[n]+\mathbf{w})\mathbf{x}^{H}[n]\mathbf{e}_{\overline{D}}] = E[(\mathbf{HCs}+\mathbf{w})\mathbf{s}^{H}\mathbf{C}^{H}\mathbf{e}_{\overline{D}}]$$

$$= \mathbf{HCR}_{\mathbf{SS}}\mathbf{C}^{H}\mathbf{e}_{\overline{D}}$$

$$= \mathbf{HCC}^{H}\mathbf{e}_{\overline{D}} \tag{3-49}$$

where autocorrelation matrix of symbols is assumed to be $\mathbf{R}_{\mathbf{SS}} = \mathbf{I}$.

Equation (3-48)and (3-49) show that equalizer is independent from the user index, however, Equation (3-44) and (3-45) underline the fact that the multiuser code matrix must be modified for equalization of each chip. The chip index dependent solution is developed in [15], [16], and [18]. On the other hand, [13] gives the simplified version of (3-48) and (3-49) and alternative adaptive solutions are proposed in [16]. In addition, the equivalence of symbol-level LMMSE and chip-level LMMSE are shown in [15] and [16]. Since the equalizer design is aimed at reducing complexity and being more practical, the simplification of the receivers given in [15], [16], and [18] is essential part of this work. The simplification of (3-48) and (3-49) can be performed as follows:

If the multiuser chip sequence is assumed to be independent identically distributed (i.i.d.) random sequence, which is used in [13] with long scrambling codes, the autocorrelation matrix of transmitted sequence can be expressed as

$$\mathbf{R}_{\mathbf{xx}} = E\left[\mathbf{x}\mathbf{x}^{H}\right] = \mathbf{C}\mathbf{R}_{\mathbf{ss}}\mathbf{C}^{\mathrm{H}} = \mathbf{C}\mathbf{C}^{H}$$

$$= K\mathbf{I} \tag{3-50}$$

where it is already assumed that $\mathbf{R}_{\mathbf{ss}} = \mathbf{I}$, and i.i.d. assumption of multiuser chip sequence results in $\mathbf{C}\mathbf{C}^{H} = K\mathbf{I}$. The coefficient in front of the identity matrix comes from the fact that $\mathbf{C}$ contains K users' unit energy chips. In the simulation results of next chapter, we will show that this result is also applicable to short periodic orthogonal codes (e.g., Walsh-Hadamard codes) if spreading factor is sufficiently large than delay spread of the channel. If also $K=N$, Walsh-Hadamard codes produce $K\mathbf{I}=N\mathbf{I}$ as previously explained in full-rank LMMSE section. It should be noted that the equivalence of the chip-level LMMSE receiver to symbol-level are valid if the code matrix is modified for each chip estimation and length of observation window is chosen as long as symbol-level case.

Substituting (3-48), (3-49) and (3-50) into (3-47) we can obtain chip-level LMMSE weight vector as

$$\mathbf{g}_{chip} = (\mathbf{H}\mathbf{H}^{\mathrm{H}} + (N_0 / K)\mathbf{I})^{-1}\mathbf{H}\mathbf{e}_{\overline{D}} \tag{3-51}$$

where noise at the input of equalizer is assumed to white.

The positive effect of estimating multiuser chip instead of desired user's chip can be seen in (3-51) with the decreased noise variance or increased SNR by K assuming that transmit power per user is kept constant.

The only parameter required for deciding observation window and optimal weight vector is delay parameter D if the equalizer order is already decided. The method of optimal delay search can be constructed as follows:

As we stated before, the optimal delay value must minimize the available MMSE expressions. The MMSE can be expressed as

$$MMSE_{chip} = K - \mathbf{g}_{chip}^{H} \mathbf{r}_{x\mathbf{y}} \tag{3-52}$$

Substituting (3-49), (3-50) and (3-51) into (3-52)

$$MMSE_{chip} = K - \mathbf{e}_{\overline{D}}^{T} \mathbf{H}^{\mathrm{H}} (\mathbf{H}\mathbf{H}^{\mathrm{H}} + (N_0 / K)\mathbf{I})^{-1} K\mathbf{H}\mathbf{e}_{\overline{D}} \tag{3-53}$$

The minimization of $MMSE_{chip}$ equals to the maximization of the $\mathbf{e}_{\overline{D}}^{T} \mathbf{H}^{\mathrm{H}} (\mathbf{H}\mathbf{H}^{\mathrm{H}} + (N_0 / K)\mathbf{I})^{-1} K\mathbf{H}\mathbf{e}_{\overline{D}}$. To make calculations simpler, we can use matrix inversion lemma and normalize the MMSE dividing by *K*. The simplified expression becomes

$$\mathbf{e}_{\overline{D}}^{T} \mathbf{B} (\mathbf{B} + (N_0 / K)\mathbf{I})^{-1} \mathbf{e}_{\overline{D}} \tag{3-54}$$

where $\mathbf{B} = \mathbf{H}^{\mathrm{H}} \mathbf{H}$. Eventually, minimization of $MMSE_{chip}$ and selection of the best delay can be completed by finding the largest diagonal element of $\mathbf{B}(\mathbf{B} + (N_0 / K)\mathbf{I})^{-1}$.

The required received sample vector for D-chip-delayed solution will become

$$\mathbf{y} = \left[y[mN + D], y[mN - 1 + D], \ldots, y[mN - L_g + D] \right] \tag{3-55}$$

where the length of the window is kept unchanged as $L_g + 1$.

The transmitted binary data of desired user can be obtained from estimated symbol of desired user $\hat{s}_k$ as

$$\hat{s}_k = \mathbf{c}_k^H \mathbf{G}_k \tilde{\mathbf{y}} \tag{3-56}$$

$$\bar{s}_k = \text{sgn}(\Re(\hat{s}_k)) \tag{3-57}$$

where $\mathbf{G}_k$ is similarly defined as $\mathbf{U}_k$, but its rows contain $\mathbf{g}_{chip}^H$ instead of $\mathbf{c}_k^H$, $\tilde{\mathbf{y}}$ is the $(L_g + N) \times 1$ observed chip sample vector spanning one symbol duration.

The performance parameters SINR and BEP of chip-level LMMSE receiver can not be calculated directly from $MMSE_{chip}$. However, they can be expressed approximately as $SINR_{chip} \approx N\left(\frac{1}{MMSE_{chip}} - \frac{1}{K}\right)$ [15], and $BEP_{chip} \approx Q(\sqrt{2SINR_{chip}})$ [13].

Finally, the solution of chip-level equalization at two limiting case can be deduced from Equation (3-51). Firstly, if the multiuser signals from different paths are assumed uncorrelated, as in the case of postdetection MRC Rake receiver, the weight vector will become approximately $\mathbf{g}_{chip} = a.\mathbf{He}_{\overline{D}}$ where a is scaling factor. Selecting equalizer order as $L_g = L_h$ and appropriate delay of $D = L_h$, this result can be considered as the solution to predetection MRC RAKE receiver, which is illustrated in Figure 3-1. Second limit can be evaluated under noiseless or high signal-to-noise ratio (SNR) case. In this case, the weight vector turns out that it has the same coefficients as ZF equalizer such that $\mathbf{g}_{chip} = (\mathbf{H}\mathbf{H}^{\mathrm{H}})^{-1}\mathbf{He}_{\overline{D}}$.

3.5. Interference-suppressing RAKE Receiver

The previously analyzed three multiuser receivers, which are conventional RAKE receiver, full-rank (symbol-level) LMMSE and chip-level LMMSE, can operate under multipath channels. However, the performance and complexity of these receivers depends on several system parameters or receiver design parameters. The conventional RAKE receiver has lowest complexity depending on channel delay spread; on the other hand, it has also worst performance when the number of active users K approaches the system capacity limited by spreading factor N. The optimal linear receiver for CDMA downlink is the full-rank (symbol-level) LMMSE receiver. However, the complexity of this optimal solution increases with larger spreading factor to accommodate additional users that should use orthogonal spreading sequences. Hence, symbol-level LMMSE is suitable for systems that use small spreading factors. For the systems that use larger spreading factor, chip-level LMMSE can be considered more applicable if the required BER is met. Because of the simplification on correlation properties of users' code, the chip-level LMMSE may not achieve the required performance level. Consequently, an appropriate solution must be developed to realize the requirement on both low-complexity and high-performance. The proposed method by [14],which is called interference-suppressing RAKE receiver, will be investigated in this section as a solution for mentioned requirements.

Two different structures of RAKE receiver given in Section 3.2 show the same performance if the weight vectors are equal. Another equivalence exists between the symbol-level and chip-level LMMSE if the equalizer lengths are chosen as equal and without any simplification on chip-level solution. These equivalences are the result of the fact that the despreading is a commutative linear operation. In addition, in Section 3.4 we conclude that the chip-level LMMSE has a similar structure to predetection (pre-filter) RAKE receiver. However, this section is established on the postdetection RAKE receiver in order to benefit from multipath diversity. Although

there exists equivalence on the linear operations applied to both RAKE receiver and chip-level LMMSE receiver, the methods of finding weight vector are different. The form of the receiver, derivation of finger coefficients and the differences in the method are explained in the subsequent parts.

The postdetection RAKE receiver, which is given in Figure 3-2, can be redrawn as in [14] to demonstrate the structure of the interference-suppressing RAKE receiver.

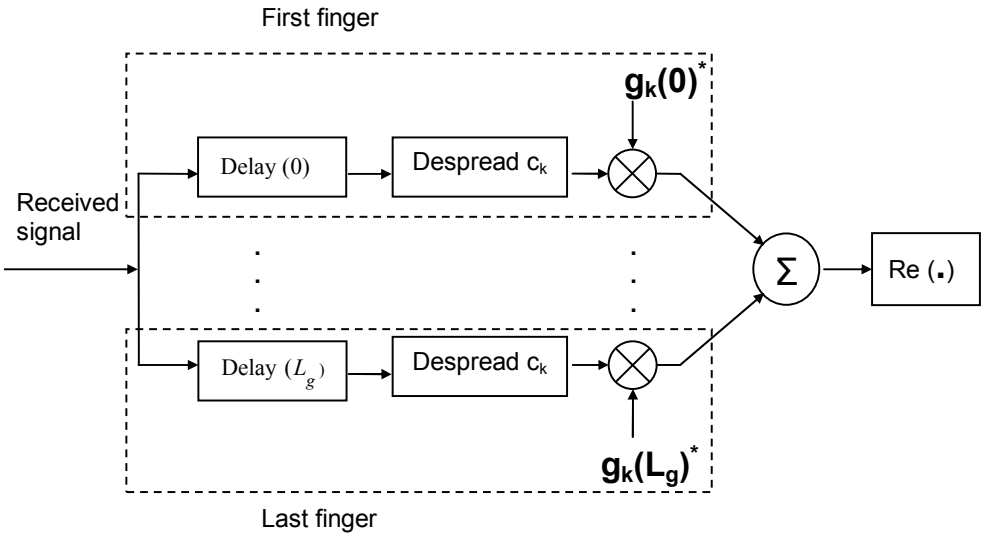

Figure 3-6: Interference-suppressing RAKE receiver

The structure of the receiver, with *k*th user's parameters and weight vector of order L_g (or L_g+1 taps), is given in Figure 3-6. The design parameters that will be used in the derivation of the receiver are number of fingers (L_g+1) and the position of the observation window D with respect to the time that first chip related to the desired

symbol. In the derivation of the finger coefficients, observation window is chosen such that $L_w = (N+L_g) \geq (N+L_h)$ to collect the signal energy from all the paths for every chip of one symbol. In other words, the effective channel seen at the output of the despreading determines the minimum length of received chip sample vector **y**. The representation of the possible observation windows given in Figure 3-5 can be also used for the interference-suppressing RAKE receiver. Hence, **y** can be constructed as

$$\begin{aligned}\mathbf{y} = \big[& y[mN-(L_h+L_g)+D], y[mN-(L_h+L_g-1)+D],\ldots, \\ & y[mN-1], y[mN], y[mN+1],\ldots, y[mN+N-1+D]\big]^T\end{aligned} \tag{3-58}$$

Since **y** can be decomposed as **y** =**HCs** + **w**, the effect of delay on the *k*th user's code matrix $\mathbf{C}_k$ can also be expressed as

$$\mathbf{C_k} = \begin{bmatrix} c_k[N-(L_g+L_h)+D] & 0 & 0 \\ c_k[N-(L_g+L_h)+1+D] & \vdots & \vdots \\ \vdots & & \\ c_k[N-2] & & \\ c_k[N-1] & 0 & 0 \\ & c_k[0] & 0 \\ 0 & c_k[1] & \vdots \\ \vdots & \vdots & \\ \vdots & c_k[N-2] & \\ & c_k[N-1] & 0 \\ & 0 & c_k[0] \\ & \vdots & \vdots \\ 0 & 0 & c_k[D-1] \end{bmatrix} \tag{3-59}$$

Note that the construction of (3-58) and (3-59) is similar to that of symbol-level LMMSE; however, different from that of chip-level LMMSE. The difficulty that

comes from the reconstruction of code matrix in chip-level LMMSE for N chip can be handled by applying estimation in symbol-level. The interference-suppressing RAKE also provides this accomplishment.

The common difference of interference-suppressing RAKE receiver from both of the equalizer type receivers is that the despreading process is directly included in the derivation of the finger coefficients. The despreading process at all branches can expressed as

$$\mathbf{z} = \mathbf{U}_k \mathbf{y} \tag{3-60}$$

Where $\mathbf{U}_k$ is $(L_g+1)\times(L_g+L_h)$ matrix, which can be defined as

$$\mathbf{U}_k = \begin{bmatrix} c_k[0] & c_k[1] & \cdots & \cdots & \cdots & c_k[N-1] & 0 & \cdots & 0 \\ 0 & c_k[0] & \cdots & \cdots & \cdots & c_k[N-2] & c_k[N-1] & \vdots & \vdots \\ \vdots & \vdots & \ddots & \vdots & \vdots & \vdots & \vdots & \vdots & 0 \\ 0 & \cdots & 0 & c_k[0] & \cdots & c_k[N-L] & c_k[N-L-1] & \cdots & c_k[N-1] \end{bmatrix}_{L\times(N+L-1)} \tag{3-61}$$

The correlator outputs are stacked into an intermediate variable vector $\mathbf{z}$. So far, the method follows the conventional RAKE. At this point, finger coefficients can be derived using correlator outputs and MSE cost criterion as follows:

$$\mathbf{g}_{k,IS-RAKE} = \arg\min_{g} E\left[\left|s_k - (\mathbf{g}^T\mathbf{z})\right|^2\right] \tag{3-62}$$

$$\hat{s}_k = \mathbf{g}_{k,IS-RAKE}^T \mathbf{z} \tag{3-63}$$

To simplify calculations real-valued variables are considered, the same relation are also applicable to complex-valued case. The output of the combiner produces the soft

decision or estimate of the desired user's symbol. The binary value of this soft decision can be calculated from complex-valued variables, simply as

$$\bar{s}_k = \text{sgn}(\Re(\mathbf{g}_{k,IS-RAKE}^H \mathbf{z})) \tag{3-64}$$

If the Equation (3-63) is expanded into its elements as

$$\begin{aligned} \hat{s}_k &= \mathbf{g}_{k,IS-RAKE}^H \mathbf{U}_k \mathbf{y} \\ &= \mathbf{g}_{k,IS-RAKE}^H \mathbf{U}_k \mathbf{HCs} + \mathbf{g}_{k,IS-RAKE}^H \mathbf{U}_k \mathbf{w} \end{aligned} \tag{3-65}$$

the linear operations applied to the transmitted multiuser symbol can be seen more apparently. However, the correlation properties of users' spreading codes should be shown more explicitly in order to achieve interference suppression.

To obtain the correlation between desired user's code and interferers' codes, the despreading operation can be applied using commutativity property of convolution operation prior to the step that multiuser chip is convolved with the propagation channel. The alternative representation given in [14] can be expressed as

$$\begin{aligned} \hat{s}_k &= \mathbf{g}_{k,IS-RAKE}^H \mathbf{U}_k \mathbf{HCs} + \mathbf{g}_{k,IS-RAKE}^H \mathbf{U}_k \mathbf{w} \\ &= \mathbf{g}_{k,IS-RAKE}^H \widetilde{\mathbf{H}}\widetilde{\mathbf{U}}_k \mathbf{Cs} + \mathbf{g}_{k,IS-RAKE}^H \mathbf{U}_k \mathbf{w} \end{aligned} \tag{3-66}$$

The existence of the equality $\widetilde{\mathbf{H}}\widetilde{\mathbf{U}}_k = \mathbf{U}_k \mathbf{H} = \mathbf{F}_k$ can be proven as follows:

Let the $\mathbf{F}_k(i, j)$ denote the element of resultant matrix $\mathbf{F}_k$, where i and j show the row and column index respectively. We can express $\mathbf{F}_k(i, j)$ as the inner product of two vector as

$$\mathbf{F}_k(i,j) = \mathbf{U}_k(i,:)\mathbf{H}(:,j)$$

where $\mathbf{U}_k(i,:)$ is ith row of $\mathbf{U}_k$ and $\mathbf{H}(:,j)$ is jth column of $\mathbf{H}$. We can continue with the element-by-element operations.

$$\mathbf{F}_k(i,j) = \sum_{r=1}^{N+L_g} c_k(r-i)h(r+L_h-j) \tag{3-67}$$

where $h[n]$ is the sequence of channel taps and zero outside $[0,L_h]$, and $c_k[n]$ is the kth user's code sequence and defined on $[0,N\text{-}1]$. By changing of variables as $r' = -r + i + j$

$$\mathbf{F}_k(i,j) = \sum_{r'} c_{\mathrm{k}}(-r'+j)h(-r'+L_h+i)$$

$$\mathbf{F}_k(i,j) = \sum_{r'=i+j-1}^{i+j-(N+L_g)} h(-r'+L_h+i)\,c_{\mathrm{k}}(-r'+j)$$

Since $h[n]$ and $c_k[n]$ are zero outside the interval $[0,L_h]$ and $[0,N\text{-}1]$ respectively, and $1 \le i \le (L_g+1)$, $1 \le j \le (L_g+L_h+N)$; we can end up with

$$\mathbf{F}_k(i,j) = \sum_{r'=1}^{L_g+L_h+1} h(-r'+L_h+i)\,c_{\mathrm{k}}(-r'+j) \tag{3-68}$$

We can use the similarity that time index proceeds in the reverse direction as in the columns of $\mathbf{U}_k$ and in the rows of $\mathbf{H}$. Finally we can write the $\mathbf{F}_k(i,j)$ and $\mathbf{F}_k$ as

$$\mathbf{F}_k(i,j) = \widetilde{\mathbf{H}}(i,:)\widetilde{\mathbf{U}}_k(:,j)$$

$$\mathbf{F}_k = \widetilde{\mathbf{H}}\widetilde{\mathbf{U}}_k$$

$$\mathbf{U}_k\mathbf{H} = \widetilde{\mathbf{H}}\widetilde{\mathbf{U}}_k$$

The new matrix $\widetilde{\mathbf{H}}$ can be constructed from $\mathbf{H}$ by taking first L_g+1 rows and first (L_g+ L_h+1) columns of $\mathbf{H}$.

$$\mathbf{H} = \begin{bmatrix} \overbrace{\begin{bmatrix} h_{L_h} & \cdots & h_0 & 0 \\ 0 & \ddots & & \ddots \\ & h_{L_h} & & h_0 \end{bmatrix}}^{\widetilde{\mathbf{H}}} & & & 0 \\ & \ddots & \ddots & \vdots \\ & & & 0 \\ & & \ddots & \vdots \\ & h_{L_h} & & h_0 \\ & & \ddots & \\ 0 & & 0 & h_{L_h} \end{bmatrix} \begin{matrix} \\ \\ \\ \\ \\ \\ \\ h_0 \end{matrix}$$

Similarly, $\widetilde{\mathbf{U}}_k$ can be derived from $\mathbf{U}_k$ by adding L_h more rows and padding upper L_g+1 rows by appropriate number of zeros. Hence, the new matrix becomes

$$\widetilde{\mathbf{U}}_k = \begin{bmatrix} \overbrace{\begin{bmatrix} c_k[0] & & c_k[N-1] & 0 & \cdots & \\ 0 & \ddots & & \ddots & & \\ \vdots & & c_k[0] & & & c_k[N-1] \end{bmatrix}}^{\mathbf{U}_k} & & & 0 \\ & \ddots & & \vdots \\ & & \ddots & \ddots & & 0 \\ 0 & \cdots & 0 & c_k[0] & & c_k[N-1] \end{bmatrix}$$

(3-62) and (3-66) can be rearranged as

$$\hat{s}_k = \mathbf{g}_{k,IS-RAKE}^H \widetilde{\mathbf{H}}\mathbf{R}_k\mathbf{s} + \mathbf{g}_{k,IS-RAKE}^H \mathbf{U}_k\mathbf{w} \tag{3-69}$$

where $\mathbf{R}_k = \widetilde{\mathbf{U}}_k\mathbf{C}$ is the desired user's code correlation matrix with respect to all the users' codes. Note that, the desired user's code correlation matrix $\mathbf{R}_k$ does not depend on the channel taps. The matrix is also independent from the symbol.

The correlator outputs are the sufficient statistics [8] for the symbol-level estimation of s_k. The combiner output given in (3-69) can be substituted into (3-17) to yield a similar expression to (3-23) that the minimization problem of MSE can be solved again by constructing Wiener-Hopf equations. The new Wiener-Hopf equations will become

$$\mathbf{R}_{\mathbf{zz}}\mathbf{g}_{k,IS-RAKE} = \mathbf{r}_{s\mathbf{z}}$$

$$\mathbf{g}_{k,IS-RAKE} = \mathbf{R}_{\mathbf{zz}}^{-1}\mathbf{r}_{s\mathbf{z}} \tag{3-70}$$

The autocorrelation matrix $\mathbf{R}_{\mathbf{zz}}$ of $\mathbf{z}$ can be represented as the product of newly defined matrices

$$\mathbf{R}_{\mathbf{zz}} = E[\mathbf{z}\mathbf{z}^{\mathrm{H}}]$$

$$= E\left[(\widetilde{\mathbf{H}}\mathbf{R}_k\mathbf{s} + \mathbf{U}_k\mathbf{w})(\widetilde{\mathbf{H}}\mathbf{R}_k\mathbf{s} + \mathbf{U}_k\mathbf{w})^H\right]$$

$$= (\widetilde{\mathbf{H}}\mathbf{R}_k\mathbf{R}_k^H\widetilde{\mathbf{H}}^H + \mathbf{U}_k\mathbf{R}_{\mathbf{ww}}\mathbf{U}_k^H) \tag{3-71}$$

The crosscorrelation between desired signal and correlator outputs can also be calculated in a similar way that we calculate it in the previous sections. However, we now use the outputs of the correlator $\mathbf{z}$ instead of received chip sample vector $\mathbf{y}$

$$\mathbf{r}_{s\mathbf{z}} = E[s_k \mathbf{z}]$$

$$= E\left[s_k (\widetilde{\mathbf{H}}\mathbf{R}_k \mathbf{s} + \mathbf{U}_k \mathbf{w})\right]$$

$$= \widetilde{\mathbf{H}}\mathbf{R}_k \mathbf{e}_{3(k-1)+2} \tag{3-72}$$

Finally, the required finger coefficients can be acquired by substituting (3-71) and (3-72) into (3-70)

$$\mathbf{g}_{k,IS-RAKE} = \mathbf{R}_{\mathbf{zz}}^{-1} \mathbf{r}_{s\mathbf{z}}$$

$$\mathbf{g}_{k,IS-RAKE} = (\widetilde{\mathbf{H}}\mathbf{R}_k \mathbf{R}_k^H \widetilde{\mathbf{H}}^H + N_0 \mathbf{U}_k \mathbf{U}_k^H)^{-1} \widetilde{\mathbf{H}}\mathbf{R}_k \mathbf{e}_{3(k-1)+2} \tag{3-73}$$

where the noise covariance matrix is replaced by $\mathbf{R}_{\mathbf{ww}} = N_0 \mathbf{I}$ since it is assumed to be white Gaussian noise.

The performance of this receiver can be evaluated by considering the following statements:

The delay parameter *D* can not be explicitly seen in (3-73) as the expression of full-rank LMMSE. Hence, the problem is also the same as that of full-rank LMMSE. The performance results varying with delay parameter are given in the next chapter.

The average performance of this MMSE based interference-suppressing RAKE (IS-RAKE) receiver can be evaluated considering two variable. First, we can calculate the MMSE from (3-72) and (3-73) as

$$MMSE_{IS-RAKE} = 1 - \mathbf{g}_{IS-RAKE}^H \mathbf{r}_{s\mathbf{z}} \tag{3-74}$$

$$MMSE_{IS-RAKE} = 1 - \mathbf{e}_{3(k-1)+2}^{H} \mathbf{R}_k^H \tilde{\mathbf{H}}^H (\tilde{\mathbf{H}} \mathbf{R}_k \mathbf{R}_k^H \tilde{\mathbf{H}}^H + N_0 \mathbf{U}_k \mathbf{U}_k^H)^{-1} \tilde{\mathbf{H}} \mathbf{R}_k \mathbf{e}_{3(k-1)+2} \quad (3\text{-}75)$$

Note that the MMSE expression for IS-RAKE given in Equation (3-75) is very similar to that of full-rank LMMSE given in (3-36). The differences are caused by the despreading operation prior to combiner. The despreading of received chip sample vector **y** with $\mathbf{U}_k$ results in that the computational complexity is reduced while the degrees of freedom required for suppressing the interference is decreased. However, the effective filter length, which is obtained by cascading the correlator and combiner, at the receiver for IS-RAKE will be (L_g+N) while that of full-rank LMMSE should be chosen around (L_h+N) due to computational complexity. Although the effective channel length of IS-RAKE is (L_g+N), its complexity is proportional to L_g, which can be seen from (L_g+1)×(L_g+1) matrix inversion in (3-73). On the other hand, the complexity of full-rank LMMSE is relatively high since we choose the parameters as (L_g+1+L_h) ≤ N ≤ (L_h+N) ≤ $L_{w,full}$ in the case that we analyzed so far.

The bit error probability (BEP) for BPSK modulation can be calculated from average SINR. The SINR of IS-RAKE can be obtained from (3-75) as

$$SINR_{IS-RAKE} = (MMSE_{IS-RAKE})^{-1} - 1 \quad (3\text{-}76)$$

It is obvious from (3-76) that the minimization of MSE is equivalent to maximization of SINR. The BEP of the receiver under Gaussian interference assumption can be obtained the same as full-rank LMMSE case

$$BEP_{IS-RAKE} = Q(\sqrt{SINR_{BPSK}}) \quad (3\text{-}77)$$

where $SINR_{IS-RAKE} = 2SINR_{BPSK}$.

CHAPTER 4

SIMULATION RESULTS

In this chapter, performances of the four multiuser CDMA downlink receivers are evaluated considering simulation results. In addition, the performances of the receivers are compared exploiting different aspects of simulations.

The parameters used in the simulations are given in Table 4-1. In addition, for the conventional RAKE receiver the number of fingers is equal to the number of the channel taps. Some other parameters used in all the simulations can be noted as follows:

- Sequences of rectangular pulses with duration of single chip are transmitted. Simulations with square root raised cosine can be found in references [13] and [14].

- The propagation channel is generated to be 3-tap Rayleigh fading channel with equal-power unit variance taps. The paths are located to delays of zero, three and eight chips, hence the order of the channel is 8 as chosen in [14]. The channel coefficients are assumed constant over 3-symbol periods.

- Since the pulse shape used in simulations is chosen rectangular with duration of single chip and channel taps are chip periodically spaced, the sampling is performed at chip-rate at the receiver side. If the wider pulses such as square root raised cosine pulses [13], [14] are transmitted through the channel with

random spaces between taps, the received signal can be oversampled to capture the energy of the transmitted pulse more [14].

- Although we assume single antenna at the receiver, if the practical difficulties of placing additional antennas on the mobiles are not considered, the multiple antennas can be included in a straightforward manner as in [13].

Table 4-1: The parameters used in the simulations

Representation	Definition	Value(s)	Description
N	Spreading Factor	64	System Parameter
K	Number of Active Users	1 to 64	System Parameter
L_h	Order of Propagation Channel	8	Channel Parameter
L_g	Order of Receiver Filter	8,16,24	Receiver Parameter for: Chip-level LMMSE, and IS-RAKE
L_r	Order of Additional Taps	8,16,24	Receiver Parameter for: Full-rank LMMSE
D	Delay in Chips	$(L_g + L_h)/2)$	Delay required for optimizing MMSE

4.1. Full-Load System with Minimum Length Receivers

In this configuration, the performances of the receivers are observed under full-load system with the minimum length of the receiver filters required for capturing all

multipaths. In addition, the effects of total interference (MAI, ICI and ISI) are investigated.

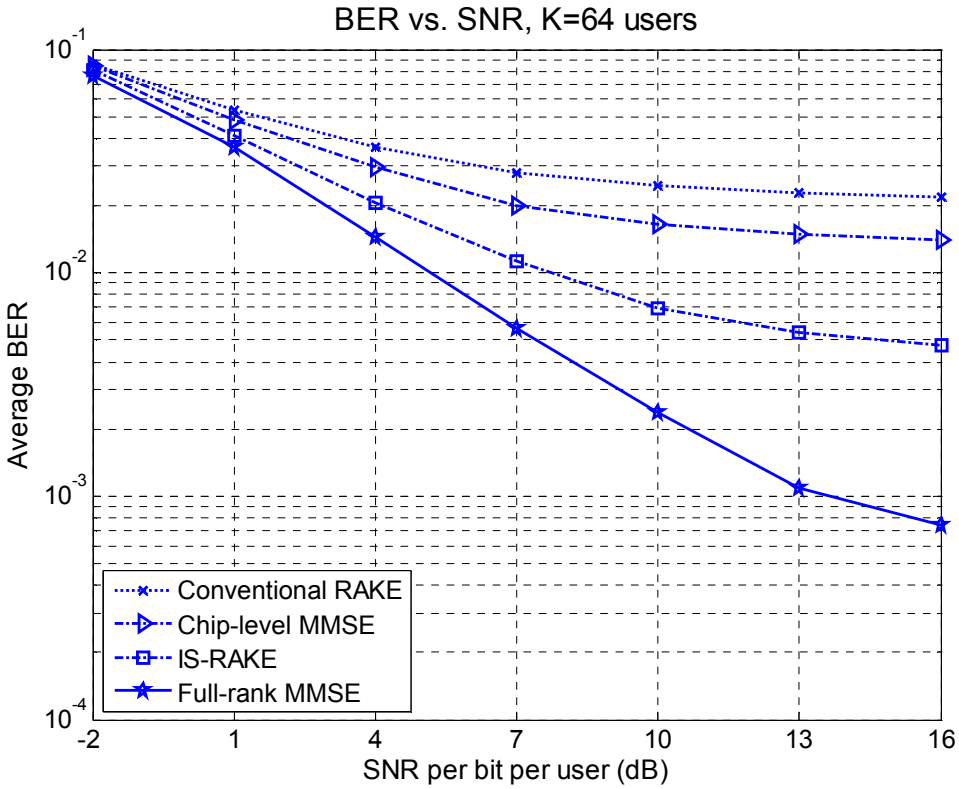

Figure 4-1: BER vs. SNR; N=K=64, $L_h = L_g = L_r$ =D=8.

The effective receiver filters can be obtained considering despreading operation. For the conventional RAKE and the IS-RAKE the effective filter can be expressed as

$$(\mathbf{g}_k^H \mathbf{U}_k)^H \tag{4-1}$$

For the chip-level LMMSE receiver it will become

$$(\mathbf{c}_k^H \mathbf{G}_k)^H \tag{4-2}$$

The effective full-rank receiver is directly obtained from $\mathbf{g}_k$ since despreading is not applied. Hence, with the parameters N=K=64, $L_h = L_g = L_r$ =D=8, the effective length of the receiver filters in chips is $N+L_g = N+L_r = N+L_h$ =72 in all receivers including conventional RAKE.

Although effective filter lengths are equal, the performance of the full-rank LMMSE receiver is significantly better than the performances of the other three receivers as seen in Figure 4-1. This is an expected result, since the degrees of freedom for selection of weight values in full-rank LMMSE are larger than the others have.

To evaluate the significance of the optimal value of D, a simulation can be performed before considering the graph of "BER vs. SNR" such that all parameters are fixed for all channel realizations but decoding is repeated varying D from 0 to $L_h + L_g$ or to $L_h + L_r$. Note that, we search for the best value of the fixed delay for reducing the time required for "BER vs. SNR" simulations, not optimize the D for each channel realization. The simulation results show that the fixed best delay D is 8 and it can be interpreted from the parameters of $L_h = L_g = L_r$ =8 as follows. Undelayed solution captures only energy from first path, to include the all the energy from 3 paths the delay is increased to 8 and kept there since available filter taps are used up. Hence, the delay parameter D is selected as 8 for three MMSE based receivers in "BER vs. SNR" simulations. The more considerable results of the delay search method are given in the following sections.

The SNR value given in the figure is the signal to noise ratio per bit per user at the input of the effective filter. As the SNR increases the slope of the BER curve

decreases since the level of interference becomes more significant than the noise level and SINR does not increases with the same rate. The chip-level LMMSE performs slightly better than the conventional RAKE and much worse than the other two MMSE based receivers do. This is caused by the insufficient equalization of the channel due to smaller number of the filter taps. Similarly, IS-RAKE tries to collect the energy from all the paths; however, interference suppression is not performed at a comparable level to full-rank LMMSE. Consequently, the performance gap between full-rank LMMSE and the other two MMSE based receiver should be reduced by increasing the length of the filters.

4.2. Performance Improvement for MMSE Receivers

As stated previous section, we can increase the length of the weight vectors to improve the performance of the receiver. On the other hand, the complexity of the receivers increases with increasing number of the taps; hence, we should determine a limit for the length of the receivers. In this section, we simulate the receivers with the parameters of $L_g = L_r = 2\,L_h = 16$ and $L_g = L_r = 3\,L_h = 24$.

4.2.1. Receiver Design with Parameters of $L_g = L_r = 2L_h = 16$

First, addition of 8 taps for all three MMSE based receiver are examined. The selection of the delay parameter D becomes more important with the parameters of $L_g = L_r = 2\,L_h = 16$ since the decision space is increased from 17 to 25.

In the "BER vs. SNR" simulation, the delay parameter D is chosen as $(L_h + L_g)/2$ by intuition. On the other hand, to verify the accuracy of the delay selection, "BER vs. Delay" simulations are performed starting with chip-level LMMSE receiver and with smaller number of channel realizations.

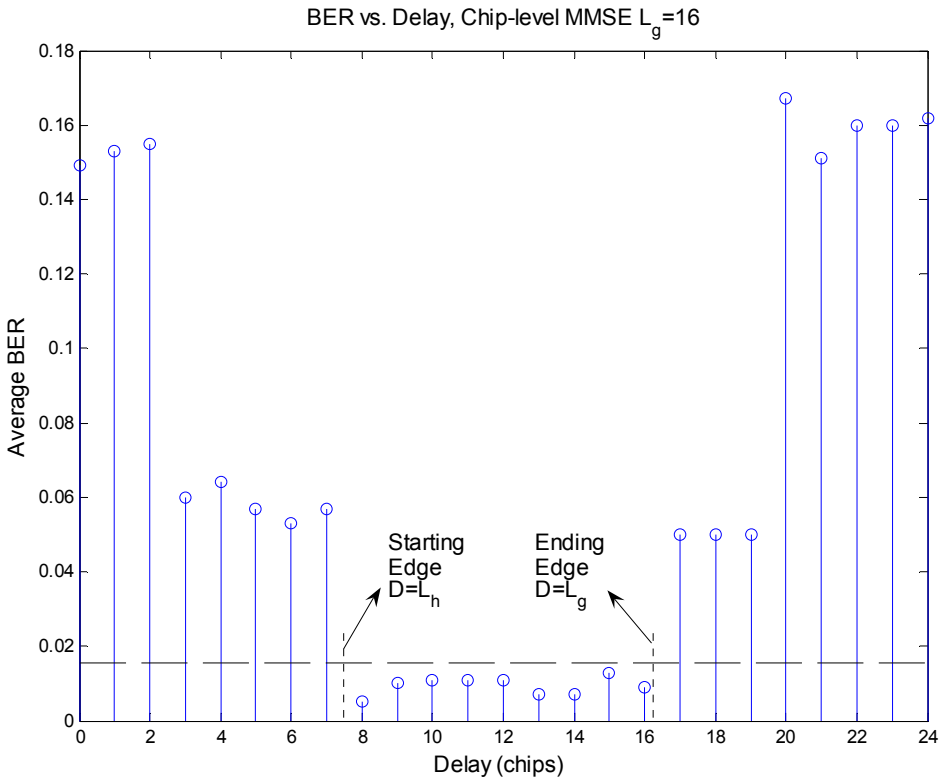

Figure 4-2: BER vs. Delay, Chip-level MMSE; N=K=64, L_h=8, L_g=16

As can be seen in Figure 4-2, the chip-level LMMSE receiver is very sensitive to the changes in the delay parameter and the receiver shows a low performance outside the range $\left[L_h, L_g\right]$. In addition, the figure reveals that $D = (L_h + L_g)/2 = 12$ is a proper selection for chip-level-LMMSE receiver.

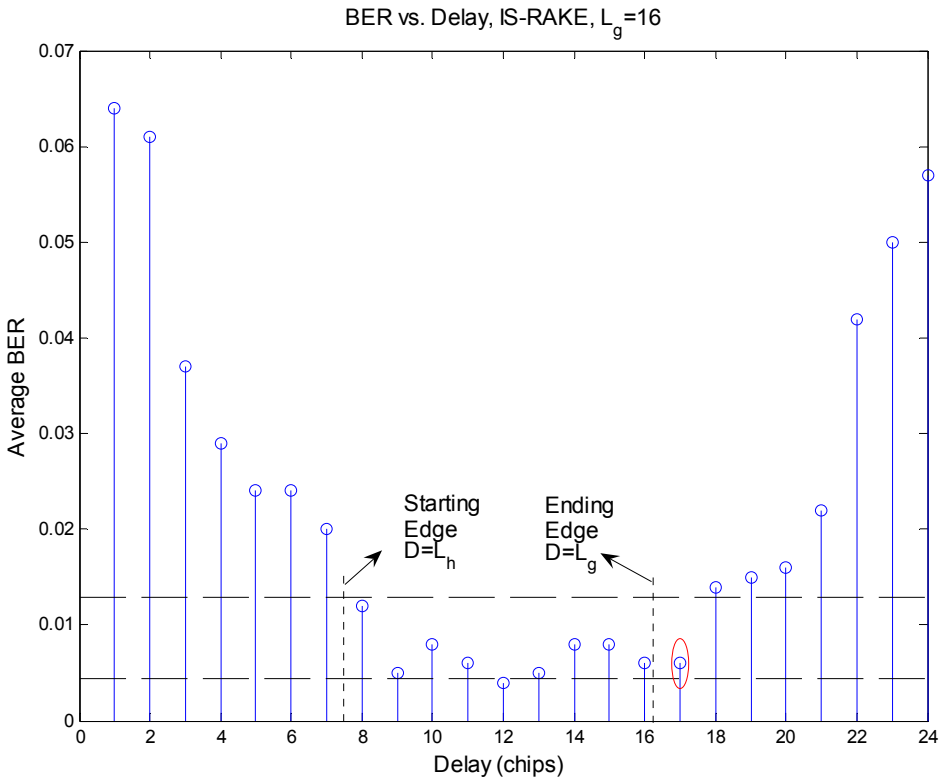

Figure 4-3: BER vs. Delay, IS-RAKE; N=K=64, L_h=8, L_g=16

As we stated in the Chapter 3, since the interference-suppressing RAKE receiver cannot be represented explicitly as a function of D, the fixed best delay is found by searching in the range $[0, L_h + L_g]$. As could be seen in Figure 4-3, the choice of the delay parameter as $D = (L_h + L_g)/2 = 12$ produces the minimum BER. Unlike the delay parameter used in the chip-level LMMSE, the delay parameter used in IS-RAKE is not restricted to the range $[L_h, L_g]$ for favorable BER result. For instance, as can be seen in Figure 4-3, the BER of D=17 is better than the BER of D=8. However, this slight difference does not change the delay selection method.

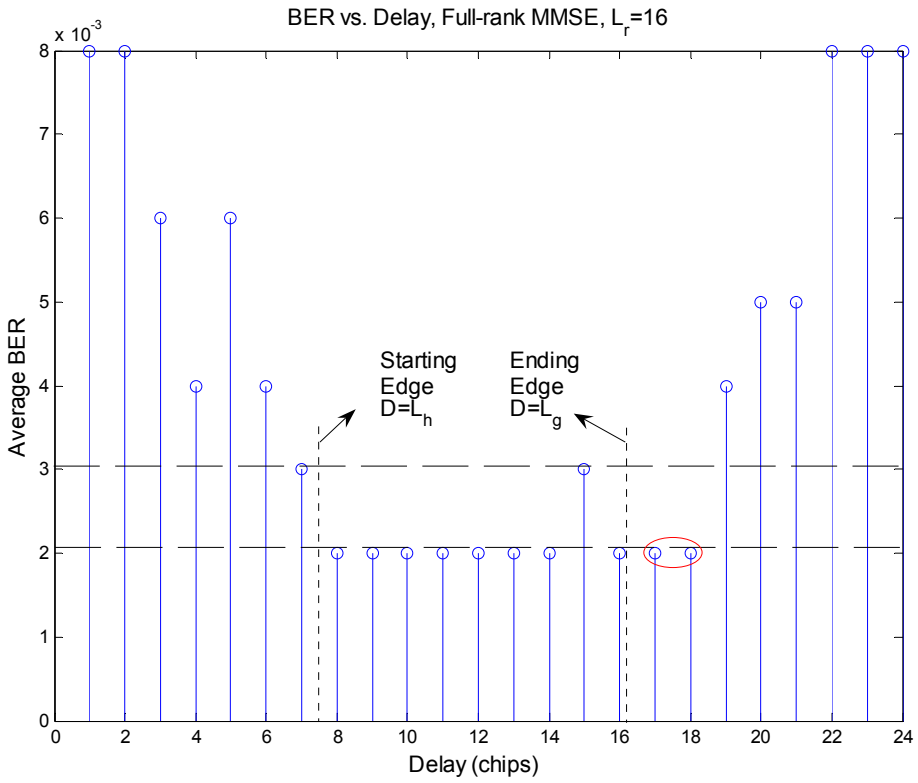

Figure 4-4: BER vs. Delay, Full-rank MMSE; N=K=64, L_h=8, L_r=16

Among three MMSE based receivers, the full-rank LMMSE shows the most stable BER results in the range $[L_h, L_g]$. As could be seen in Figure 4-4, the full-rank LMMSE is less sensitive to the changes in the delay such that the performance of the receiver in the entire interval $[0, L_h + L_g]$ is close to the BER result with the choice of $D = (L_h + L_g)/2 = 12$. Consequently, again we conclude that the delay parameter can be chosen as $D = (L_h + L_g)/2$.

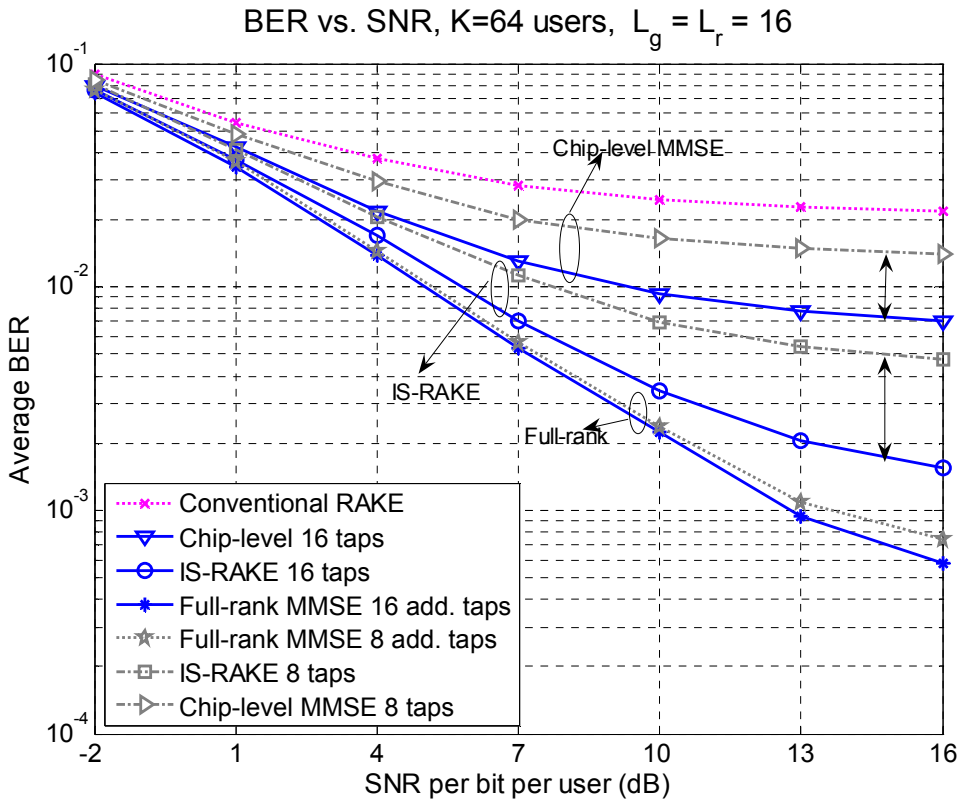

Figure 4-5: BER vs. SNR; N=K=64, L_h=8, $L_g = L_r$=16, D=12.

The performances of the receivers under full-load system with the parameters of $L_g = L_r$=2 L_h=16, and $D = (L_h + L_g)/2 = 12$ are given in Figure 4-5. As can be seen in the figure, IS-RAKE has more improvement than the others do. While the performance of the IS-RAKE with 16 taps approaches to that of the full-rank with L_r=8, the chip-level LMMSE with 16 taps has a moderate improvement in BER. On the other hand, the full-rank LMMSE, has a slight increase in its performance. Consequently, the filter lengths of both IS-RAKE and chip-level LMMSE should be increased so that at least the performance of the full-rank method with L_r=8 can be achieved.

4.2.2. Receiver Design with Parameters of $L_g = L_r = 3L_h = 24$

In this section, the results of the simulations with the parameters $L_g = L_r = 3\,L_h = 24$ and $K=N=64$ are presented. The fixed best delay search results of the three MMSE based receivers as follows:

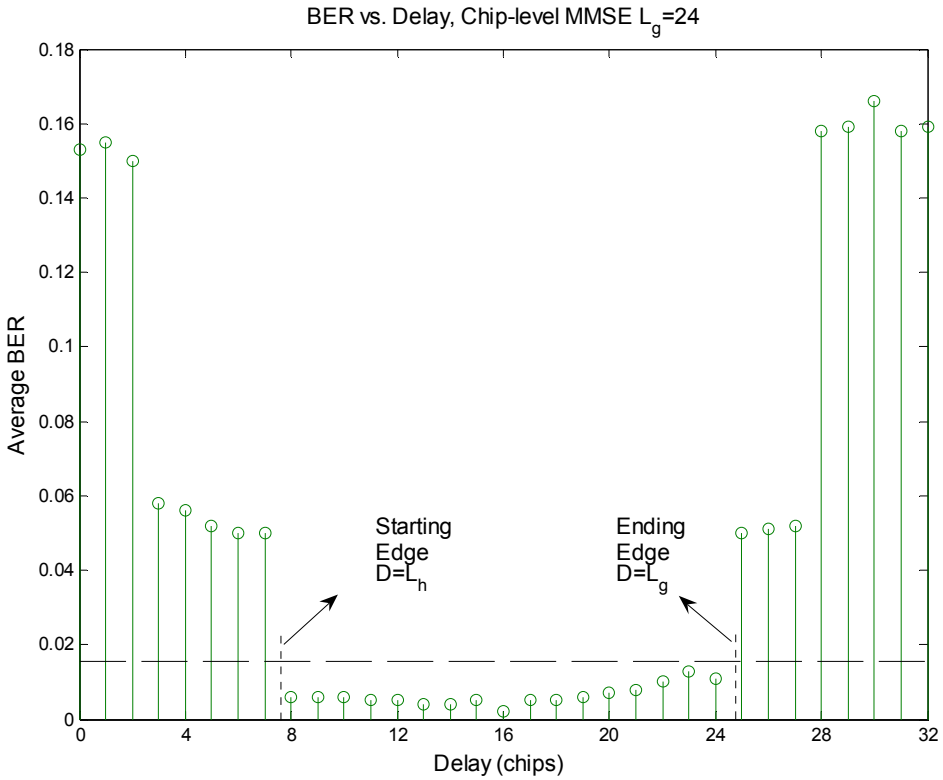

Figure 4-6: BER vs. Delay, Chip-level MMSE; $N=K=64$, $L_h=8$, $L_g=24$

As could be seen in Figure 4-6, the fixed best delay of the chip-level LMMSE with 24 taps is found $D = (L_h + L_g)/2 = 16$ as expected.

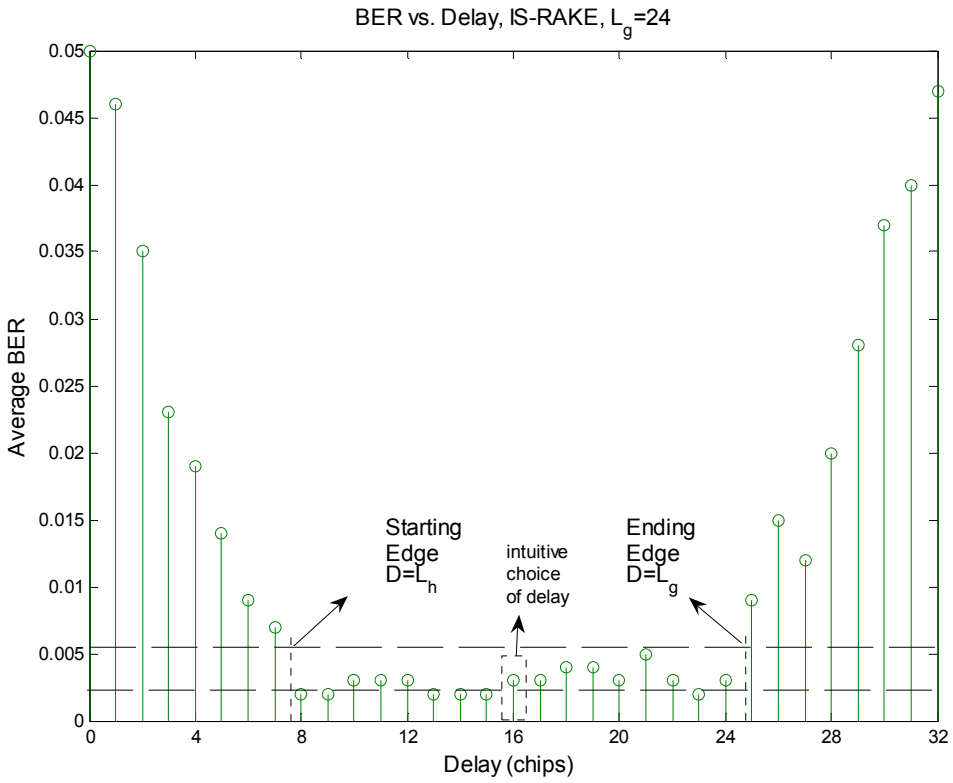

Figure 4-7: BER vs. Delay, IS-RAKE; N=K=64, L_h=8, L_g=24

In this case as can be seen in Figure 4-7, the BER of the IS-RAKE at the delay of $D = (L_h + L_g)/2 = 16$ is slightly higher than the some other delay values between L_h and L_g. Note that, again there is no small BER outside the range $[L_h, L_g]$ and $D = (L_h + L_g)/2 = 16$ is a proper choice of the delay.

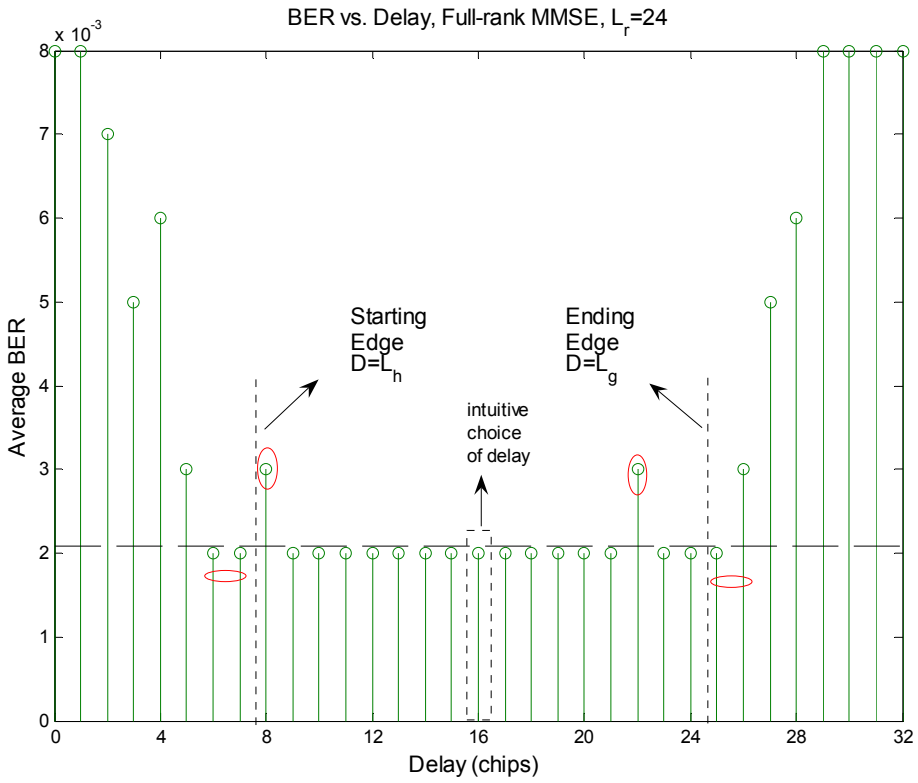

Figure 4-8: BER vs. Delay, Full-rank MMSE; N=K=64, L_h=8, L_r=24

In contrast to both IS-RAKE and chip-level LMMSE, the full-rank LMMSE has some small BER values outside the range $[L_h, L_g]$ as can be seen in Figure 4-8. The full-rank LMMSE receiver produces a flat BER curve between L_h and L_g except at delay of 8 and at delay of 22. If the delay parameter is selected somehow outside the interval $[L_h, L_g]$, the performance of the full-rank LMMSE receiver does not degrade dramatically as in the case of the chip-level LMMSE. Hence, the fixed delay parameter does not play a considerable role in the performance of the full-rank method.

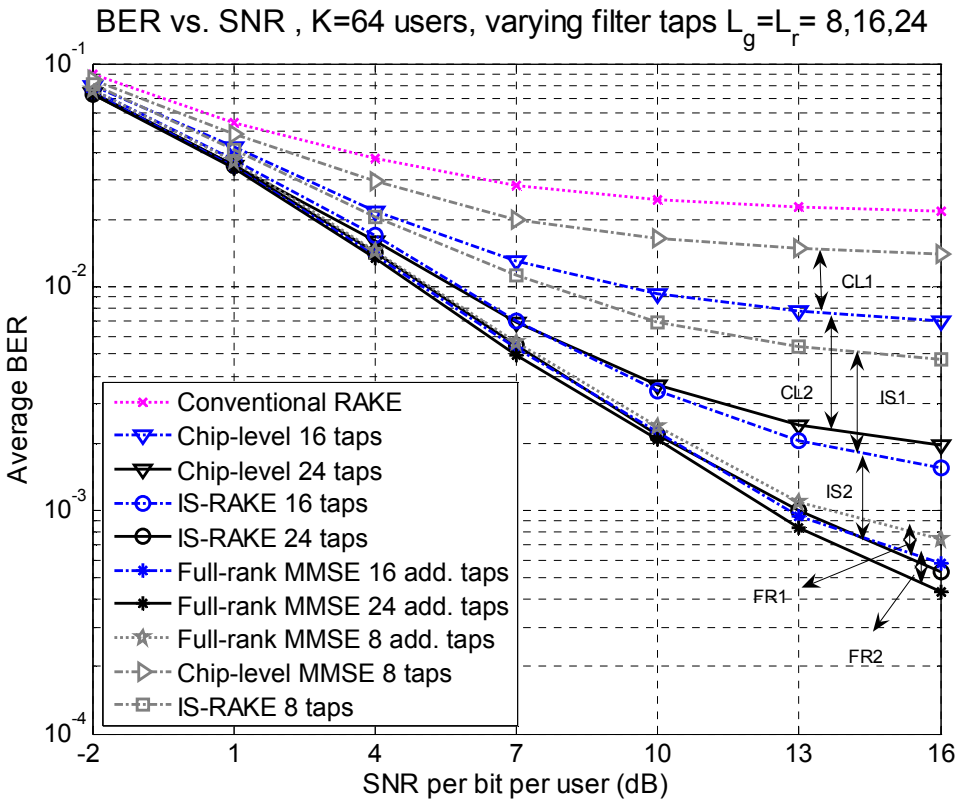

Figure 4-9: BER vs. SNR, varying number of filter taps; N=K=64, L_h=8

As could be seen in Figure 4-9, the three MMSE based receiver continue to improve the BER performance as the number of receiver taps increases. The most considerable result of this simulation is that the IS-RAKE with 24 taps approaches the performance of the full-rank LMMSE with 24 additional taps and outperforms the full-rank LMMSE with L_r=8 and L_r=16. The improvements of the IS-RAKE are shown in the figure with double arrows labeled "IS1" and "IS2". This is not a surprising result remembering that the total length of the IS-RAKE becomes $N+L_g$ = 88, which is larger than both full-rank LMMSE $N+L_r$ = 72 with L_r=8 and full-rank LMMSE $N+L_r$ = 80 with L_r=16. On the other hand, the chip-level LMMSE receiver

shows more improvement relative to the initial condition as illustrated in Figure 4-9 with double arrows labeled “CL1” and “CL2”. Although the chip-level LMMSE shows a significant improvement with increasing filter length, the performance of the chip-level method with L_g=24 is still far away from the performance of the full-rank method with L_r=8. Furthermore, the performance of the chip-level MMSE receiver with L_g=24 is at a comparable level to the performance of the IS-RAKE with L_g=16. Also, the slight improvements of the full-rank LMMSE are shown in the figure with double arrows labeled “FR1” and FR2”.

The “BER vs. SNR” graphs show that all the MMSE based receivers perform slightly better than the conventional RAKE receiver at low SNR values since the noise level becomes more significant and the effect of the MAI becomes relatively small at low SNR values. Also, note that the interference suppressing ability of the MMSE based receivers can be shown more clearly at moderate SNR values and at high SNR values.

As a final remark of this section, the performance of the chip-level LMMSE receiver may approach to full-rank method if the length of the filter is increased to an order of the spreading gain *N*. However, this is not performed since the complexity of the receiver exceeds an acceptable level and this situation contradicts with low-complexity MMSE receiver requirements. On the other hand, the performance of the IS-RAKE with meets L_g=24 the performance of the full-rank method with L_r=8 and L_r=16 and approaches to the performance of the full-rank LMMSE with L_r=24. Hence, there is no need to increase the filter length of the IS-RAKE receiver if the receiver runs at nearly its full-load.

4.3. BER vs. the Number of the Active Users

In this section, another aspect of the multiuser CDMA communication is investigated. The user capacity of the receivers concerned in this thesis for a required BER is the objective of this section. The capacity of the receivers for a target BER can be seen in Figure 4-10. The generation of the figure is based on averaging BER values of many users and realizing different Rayleigh fading channels many times that channel properties are defined at the beginning of this chapter. The SNR per chip value used in this figure is -14 dB or SNR per symbol is $-14+10\log_{10}(64) = 4$ dB.

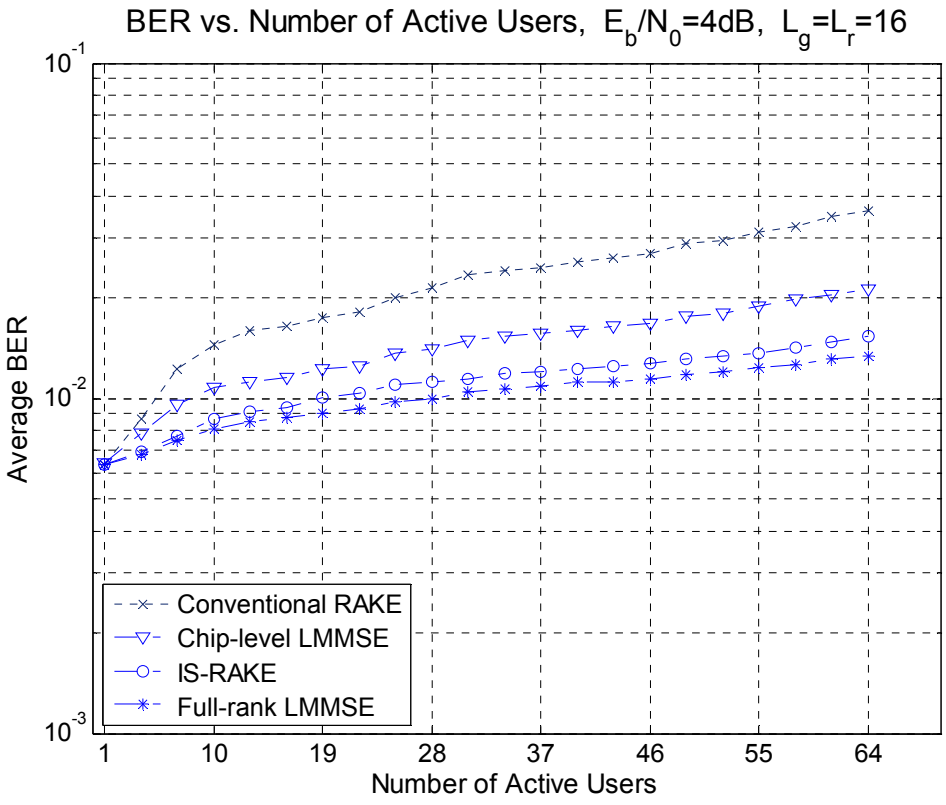

Figure 4-10: BER vs. No. of Active Users; *SNR*=4dB, N=64, L_h=8, $L_g = L_r$=16

As could be seen in Figure 4-10, the performance gap between MMSE based receivers and the conventional RAKE receiver increases as the number of the active users increases. Although the simulation is performed at a SNR value that can be considered as moderate relative to the processing gain, the performance of the receivers shows a slowly decreasing trend since the users' codes become uncorrelated and the relation between the transmitted symbols approaches the independent Gaussian approximation.

The performances of the receivers are also evaluated at higher SNR values. First, it is shown that the performance differences of the receivers increases by increasing E_b/N_0 to 10 dB in Figure 4-11

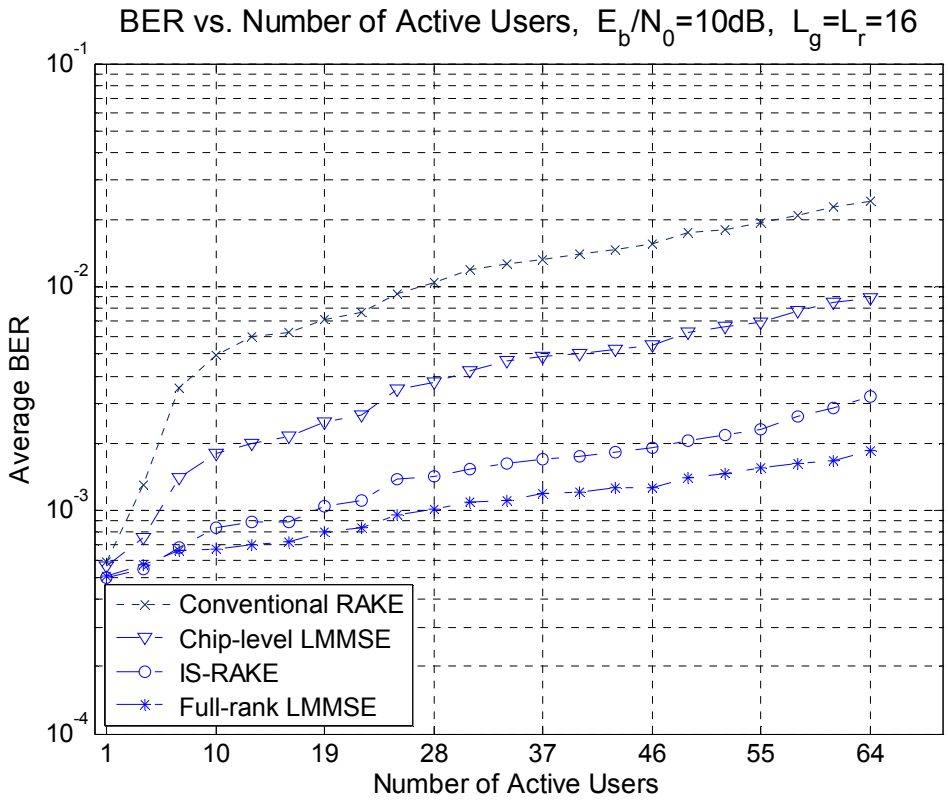

Figure 4-11: BER vs. No. of Active Users; *SNR*=10dB, N=64, L_h=8, $L_g = L_r$=16

When the SNR is set to E_b/N_0 =16 dB, the performance gap between MMSE based receivers and conventional RAKE receiver becomes more apparent as in Figure 4-12.

As a result, the IS-RAKE is more likely to improve its performance since the desired user's code and the codes of the interfering users are directly included in the derivation of the weight vector of the filter. Although the despreading can commute over the receiver filter due to its linearity, the performance of the different receivers that use the despreading in different order may be quite dissimilar. Hence, the operation order of the despreading plays an important role in the receiver performance since it has a considerable effect on the weight vector calculations.

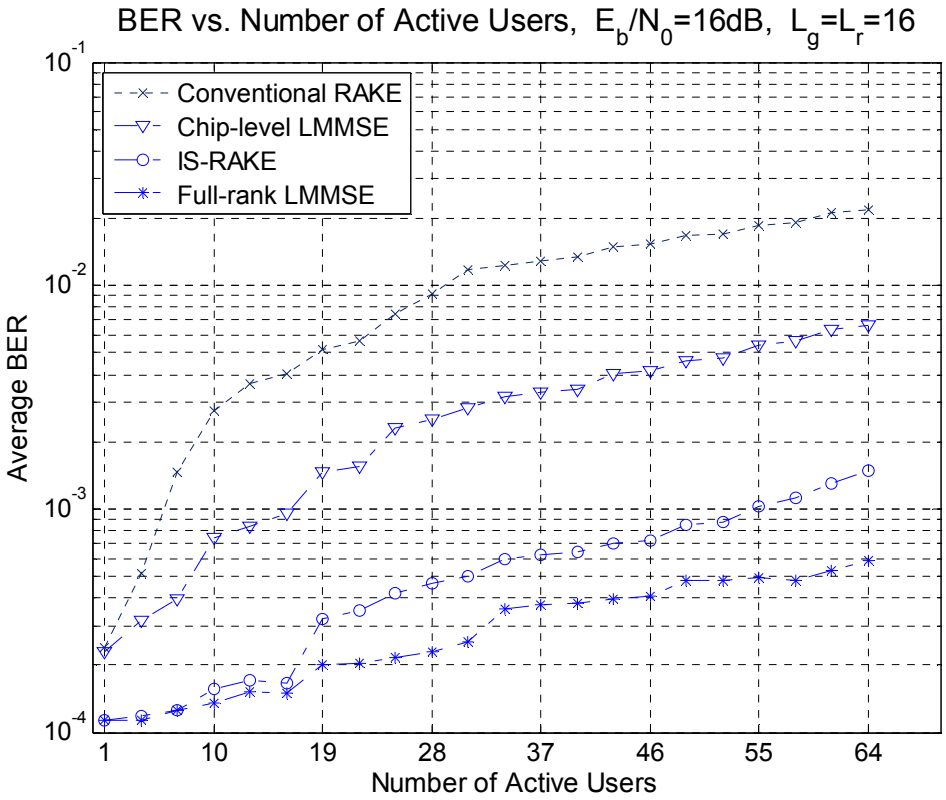

Figure 4-12: BER vs. No. of Active Users; *SNR*=16dB, N=64, L_h=8, $L_g = L_r$=16

CHAPTER 5

CONCLUSIONS

CDMA is a multiple-access technique that offers many advantages to multiuser wireless communication. Properties of CDMA system can be categorized as natural robustness to narrowband interference because of using spread-spectrum signals, global frequency reuse provided that out-of-cell interference is made negligible in transmission or at the receiver, multiple-access interference (MAI) suppression utilizing orthogonal spreading codes and/or pseudo-random spreading codes, and suppressing the interference caused by multipath propagation (or frequency-selective) channel. The latter two of the stated properties are investigated in the scope of this thesis work.

In this thesis work, four multiuser receivers for the CDMA downlink are examined considering different aspects of CDMA downlink communication. In Chapter 2, a general mathematical model of the CDMA downlink is constructed so that the receivers can be analyzed more accurately and the performances of the different receivers can be fairly evaluated.

In Chapter 3, the analysis of the four receivers is presented using common system and signal model constructed in Chapter 2. The first receiver presented in Chapter 3 is the conventional RAKE receiver. The postdetection MRC RAKE receiver maximizes the energy of the desired user. MRC RAKE tries to match both desired user's spreading sequence and the channel coefficients. The conventional RAKE receiver is considered as a low-complexity receiver with an acceptable performance

in moderately loaded communication channels. A moderately loaded system has the ratio of number of active users to spreading factor around $K / N \approx 0.2$. However, the performance of the conventional RAKE is significantly reduced for the communication channels with large number of users and having a large delay spread. Secondly, the optimal linear symbol-level receiver, which is also called full-rank LMMSE, is derived applying MSE criterion. The minimization of the MSE is performed on an observation window, which is sufficiently large to cover a symbol period and signals from all the paths related to that symbol. In contrast to the conventional RAKE, the full-rank LMMSE receiver does not perform despreading operation since the optimal solution makes use of maximum degrees of freedom to eliminate the symbol MSE. However, this method requires a large number of unknowns to be found, therefore requires significant computational power. The complexity of the receiver increases with a rate proportional to the third power of the minimum of the spreading gain or the number of the active users. Due to practical reasons, it is desired to have a lower-complexity receiver with a performance better than the conventional RAKE and a comparable performance with LMMSE receiver.

The first alternative method for satisfying acceptable complexity and performance is the chip-level LMMSE, which is presented in Section 3.4. This method applies channel equalization at chip-level and then uses despreading operation to obtain the estimate of the desired symbol. The chip-level LMMSE has an acceptable complexity such that the matrix and vector sizes are proportional to the delay spread. This method uses the assumption of ideal spreading codes for all users. The cascade of chip-level equalization filter and despreading operation forms an effective filter, which is suboptimal in comparison with full-rank LMMSE.

The second low-complexity receiver, which is an MMSE based interference-suppressing RAKE receiver, is studied in Section 3.5. In this section, it is shown that the interference-suppressing RAKE receiver both achieves symbol-level estimation

and benefits from the knowledge of the users' code without increasing the complexity as in the case of the full-rank LMMSE.

In Chapter 4, we have evaluated the performance of four multiuser receivers by simulating the CDMA downlink, which is modeled in Chapter 2. The performance results are obtained by varying SNR per chip, the number of the taps used in the MMSE based receivers (the number of the fingers for conventional RAKE receiver is set to channel length as usual) and the number of the active users.

The "BER vs. SNR" simulations show that the performance difference between the conventional RAKE receiver and the full-rank LMMSE can be managed by gradually increasing the filter lengths of two low-complexity MMSE based receivers. As a part of the minimization problem, the fixed best delay for the observation window is calculated with the help of the simulation results.

It is also stated that the operation order of the despreading has also a significant effect on the performance of the receiver. Since the desired user's code and the codes of the interferers are included in the derivation of the weight vector, IS-RAKE shows better performance than the chip-level LMMSE does. The performance analysis of the receivers is also performed under varying system load. The "BER vs. number of active users" simulation shows that the MMSE based receivers significantly outperforms the conventional RAKE receiver.

As a result, the performance improvement in the MMSE based receivers can be considered sufficient for many practical systems while the low-complexity requirements are still provided.

REFERENCES

[1] A. J. Viterbi, "*CDMA: Principles of Spread Spectrum Communication*," Reading, MA: Addison-Wesley, 1995.

[2] D. Torrieri, "*Principles of Spread-Spectrum Communication Systems*," New York: Springer, 2005.

[3] S. Verdu, "*Multiuser Detection*," New York: Cambridge University Press, 1998.

[4] A. Goldsmith, "*Wireless Communications,*" New York: Cambridge University Press, 2005.

[5] A. S. Willsky, and G. W. Wornell, "*Course Notes: Stochastic Processes, Detection and Estimation,*" Massachusetts Institute of Technology.

[6] M. Simon, and M.-S. Alouini, "*Digital Communication over Fading Channels A Unified Approach to Performance Analysis,*" New York: Wiley, 2000.

[7] U. Madhow, and M. L. Honig, "MMSE Interference Suppression for Direct-Sequence Spread-Spectrum CDMA," *IEEE Trans. On Communications*, vol. 42, Issue 12, pp. 3178-3188, December 1994.

[8] J. R. Barry, E. A. Lee, and D. G. Messerschmitt, "*Digital Communication,*" 3rd ed., Boston: Kluwer Academic Publishers, 2004.

[9] S. Lee, "*Spread Spectrum CDMA : IS-95 and IS-2000 for RF Communications,*" New York: McGraw-Hill, 2002.

[10] Y. Selen, and E. G. Larsson , "RAKE Receiver for Channels with a Sparse Impulse Response*," IEEE Trans. on Wireless Communications*, vol. 6, Issue 9, pp. 3175-3180, September 2007.

[11] H. Sui, E. Masry, and B. D. Rao , "RAKE Finger Placement for CDMA Downlink Equalization," *Proc. IEEE Int. Conf. on Acoustics, Speech, and Signal Processing*, vol. 3, pp. 905–908, March 2005.

[12] M. Honig, and M. K. Tsatsanis , "Adaptive Techniques for Multiuser CDMA Receivers," *IEEE Signal Process. Mag.*, vol.17, Issue 3, pp. 49-61, May 2000.

[13] T. P. Krauss, M. D. Zoltowski, and G. Leus , "Simple MMSE Equalizers for CDMA Downlink to Restore Chip Sequence:Comparison to Zero-Forcing and RAKE," *Proc. IEEE Int. Conf. on Acoustics, Speech, and Signal Processing,* vol. 5, pp. 2865-2868, 2000.

[14] S. Mudulodu, G. Leus, and A. Paulraj , "An Interference-Suppressing RAKE Receiver for the CDMA Downlink," *IEEE Signal Processing Letters*, vol. 11, Issue 5, pp. 521-524, May 2004.

[15] H. Sui, E. Masry, B. D. Rao, Y. C. Yoon , "CDMA Downlink Chip-level MMSE Equalization and Finger Placement," *Conference Record of the Thirty-Seventh Asilomar Conf. on Signals, Systems and Computers*, vol. 1, pp. 1161-1165, Nov. 2003

[16] K. Hooli, M. Juntti, M. J. Hekkilä, P. Komulainen, M. Latva-aho, and J. Lilleberg , "Chip-level Channel Equalization in WCDMA Downlink," *EURASIP Journal on Applied Signal Process.,* vol. 2002, Issue 8, pp. 757-770, 2002.

[17] H. L. Van Trees, "*Detection, Estimation, and Modulation Theory*," New York: John Wiley & Sons, 2001.

[18] I. Ghauri, and D. T. M. Slock , "Linear Receivers for the DS-CDMA Downlink Exploiting Orthogonality of Spreading Sequences," *Conference Record of the Thirty-Second Asimolar Conf. on Signals, Systems & Computers*, vol. 1, pp. 650-654, November 1998.

[19] G. Bottomley, T. Ottosson, and Y.-P. E. Wang , "A Generalized RAKE Receiver for Interference Suppression," *IEEE Journal on Selected Areas in Communications*, pp. 1536-1545, Aug. 2000.

[20] M. H. Hayes , "*Statistical Digital Signal Processing and Modeling*," New York: John Wiley & Sons, 1996.

[21] X. Wang and H. V. Poor, "Space-time multiuser detection in multipath CDMA channels," *IEEE Trans. on Signal Processing*, vol. 47, pp. 2356–2374, Sept. 1999.

[22] M. K. Tsatsanis, and Z. Xu , "Performance Analysis of Minimum Variance CDMA Receivers," *IEEE Trans. on Signal Processing,* vol. 46, Issue 11, pp. 3014-3022, Nov. 1998.

[23] S. Gezici, M. Chiang, H.V. Poor, and H. Kobayashi, "Optimal and Suboptimal Finger Selection Algorithms for MMSE RAKE Receivers in Impulse Radio Ultra-Wideband Systems," *Eurasip Journal on Wireless Communications and Networking*, vol. 2006, pp.1-10, 2006.